Recyclable Mesoporous Organosilica Nanoparticles Derived from Proline-Valinol Amides for Asymmetric Organocatalysis

Hao Li, Míriam Pérez-Trujillo, Xavier Cattoën, Roser Pleixats

Recyclable mesoporous organosilica nanoparticles derived from proline-valinol amides for asymmetric organocatalysis

Hao Li,[†] Míriam Pérez-Trujillo,[#] Xavier Cattoën,[§] and Roser Pleixats[†]*

†Department of Chemistry and Centro de Innovación en Química Avanzada (ORFEO-CINQA), Faculty of Sciences, Carrer dels Til.lers, UAB Campus, Universitat Autònoma de Barcelona, 08193-Bellaterra (Cerdanyola del Vallès), Barcelona, Spain. E-mail: roser.pleixats@uab.cat

NMR Service, Faculty of Sciences, Carrer de la Vall Moronta, UAB Campus, Universitat Autònoma de Barcelona, 08193-Bellaterra (Cerdanyola del Vallès), Barcelona, Spain.

§ Institut Néel, 25 avenue des Martyrs, CNRS and Université Grenoble-Alpes, 38042-Grenoble, France.

KEYWORDS: asymmetric aldol reaction, catalyst recycling, mesoporous silica nanoparticles, organocatalysis, sol-gel process.

ABSTRACT. Going a step further from bulk organosilicas to nanosized materials, we describe herein the preparation of mesoporous organosilica nanoparticles derived from mono- and bis-silylated proline-valinol amides, both by grafting on preformed mesoporous silica

nanoparticles (MSN) and by a co-condensation method in neutral medium using Brij-56/CTAB as templates. This is the first report on the obtention of functionalized MSN by a co-condensation procedure with a structurally complex chiral precursor. The functionalized MSN have been characterized by elemental analysis, ^{29}Si and ^{13}C CP MAS NMR, transmission electron microscopy, scanning electron microscopy, N_2-sorption measurements, dynamic light scattering, zeta-potential and powder X-ray diffraction. We have evaluated the activity of these materials as recyclable catalysts in the asymmetric aldol reaction. The best organocatalysts are those derived from the monosilylated precursor, observing good diastereo- and enantiomeric ratios with a simple and environmentally friendly optimized protocol (water, 0 ºC, absence of co-catalyst). The nanocatalyst was easily recovered by centrifugation and recycled up to five runs without loss of activity and selectivity. The use of organosilica nanoparticles reduces the problems of diffusion and low reaction rates encountered with bulk organosilicas.

INTRODUCTION

Organocatalysis constitutes an eco-friendly and cost-effective methodology for fine-chemical synthesis, avoiding the presence of metal traces which are a real concern in pharmaceutical industry. In particular, asymmetric organocatalysis[1] for the synthesis of valuable enantiomerically enriched building blocks has witnessed a tremendous progress in the past two decades. The availability of small organic molecules in optically active form, such as naturally abundant and low-cost amino acids, has enabled the induction of chirality in a wide range of carbon-carbon bond forming reactions.[2-26] The advantages of asymmetric organocatalysis over asymmetric transition-metal based catalysis (simple handling and storage, inertness towards oxygen and moisture, ready availability, robustness, non-toxicity, no metal contamination) have triggered the interest of some researchers for the preparation of drugs and natural bioactive compounds using metal-free procedures.[27,28]

The asymmetric direct aldol reaction is one of the most useful organic transformations, leading to the formation of new C-C bonds with the creation of one or more stereogenic centres in a diastereo- and enantioselective manner.[29,30] The amino acid L-proline and other proline derivatives have been used as organocatalysts for enantioselective aldol reactions via an enamine pathway,[17,23,29,30] often enabling the reactions to be performed in water as a sustainable medium.[31,32] Amongst the proline mimetics, Liu and Li have described novel dipeptide derivatives based on the proline catalysis concept and double hydrogen bonding activation. These authors have found that proline-valinol thioamides exhibit good to excellent activity and stereoselectivity for direct aldol reactions in the presence of acid additive.[33]

Despite the mentioned sustainable benefits of organocatalysis, the preparation of more complex organic catalysts may involve several steps, the organocatalyzed reactions often require high catalyst loadings (up to 30% molar), and the usual tedious chromatographic work-up to separate the catalyst from the reaction mixture remain as drawback. A simple strategy to facilitate easy recovery and recycling is the attachment of organocatalysts on solid organic or inorganic polymeric supports.[34-44] The formation of organic-inorganic hybrid silica materials is attractive as a means to achieve supported catalysts, as they combine the advantages of a silica matrix (high surface area, thermal and mechanical stability and presumed chemical inertness) with the properties of the organic moiety.[45,46] The sol-gel hydrolytic condensation of organoalkoxysilanes[47] is a convenient method for the preparation of organically-modified mesoporous silicas.

The applications for mesoporous organosilicas are still limited by the lack of control of the morphology and particle size. The ability to obtain nano-sized silica particles in a controlled manner broadens the spectra of applications[48-52] and improves the performances of these nanomaterials with unique properties, such as tunable monodisperse particle diameter (50-200

nm), tunable pore size (2-4 nm) and high surface areas (800-1000 m^2g^{-1}). Mesoporous silica nanoparticles (MSN) are also readily prepared by classical sol-gel techniques using cationic surfactants as templates.[53] Their nanometric size provides the advantages of an enhanced surface over volume ratio and a shorter pore length, thus easier diffusion in the case of mesoporous MCM-41 silica nanoparticles. Their short channels can act as the solid supports for highly accessible active sites in catalysis. In contrast to insoluble mesoporous organosilicas in micrometer or larger dimensions, well-suspended stable solutions of mesoporous organosilica nanoparticles should provide higher reaction rates in catalytic processes. The functionalization of MSN with organic groups can be carried out after the synthesis of the nanomaterial (post-grafting)[54] or, alternatively, by co-condensation with the required functionalized silylated compound.[55] However, including large amounts of organosilanes during the synthesis of MSNs often leads to important morphological and textural modifications. The co-condensation procedure with complex molecules remains thus a challenging task. On the other hand, dense silica nanoparticles can also be easily obtained either by the Stöber method or by reverse microemulsion.[53]

In spite of the potential of organically modified MSN, they have scarcely been applied in organocatalysis. Most of the examples involve simple achiral organocatalysts for aldol,[56-58] Knoevenagel,[59,60] and Henry condensations,[56,57,61-63] Michael additions,[64] cyanosilylation[56] and Diels-Alder[65] reactions, conversion of cellulose to 5-hydroxymethylfurfural,[66] synthesis of tetrasubstituted imidazoles by a four component reaction,[67] selective formation of enol lactones and δ-keto esters from chromene and formic acid,[68] and one-pot three-component synthesis of 2-aminochromene derivatives.[60] As far as the asymmetric organocatalysis is concerned, only chiral imidazolidinones on mesoporous silica nanoparticles obtained by post-synthesis procedures have been described for stereoselective Diels-Alder cycloadditions.[69]

Following our studies on recyclable organocatalysts[70-75] based on sol-gel methodologies, and in a step further from bulk insoluble organosilicas to dispersible nanosized materials, we present herein our results concerning the preparation of mesoporous silica nanoparticles derived from mono- and bis-silylated proline-valinol amides, as well as their activity and recyclability in the asymmetric direct aldol reaction. We have used both post-grafting and co-condensation methods. For the best of our knowledge, this is the first report on asymmetric induction on this reaction achieved by mesoporous silica nanoparticles derived organocatalysts.

RESULTS AND DISCUSSION

Preparation and characterization of mesoporous silica nanoparticles derived from proline-valinol amides.

A mono- and a bis-silylated proline-valinol amide precursors **P1** and **P2** were envisaged for the preparation of functionalized mesoporous silica nanoparticles. The synthesis of **P1** was performed from commercially available N-benzyloxycarbonyl-4-trans-hydroxy-L-proline **1**, as depicted in Scheme 1 (four steps, 79% overall yield from **1**). An initial double propargylation[76] of **1** in the presence of sodium hydride and excess of propargyl bromide provided **2** in 81% yield. The subsequent hydrolysis of the ester[76] by using aqueous sodium hydroxide in methanol gave the free acid **3** in 93% yield after acidic work-up. A better alternative consists in the direct obtention of acid **3** from **1** in 88 % yield by chemoselective O-alkylation.[77] The amide **4** was prepared in 94% yield, through the intermediacy of a mixed anhydride, by reaction with L-valinol in the presence of triethylamine.[33] A copper-catalyzed alkyne azide cycloaddition reaction (CuAAC)[78,79] of the alkyne **4** with (3-azidopropyl)-triethoxysilane **5** under anhydrous conditions[80] provided quantitatively the dipeptide **6**. The best results in our case were obtained

with the use of CuI and tris(benzyltriazolylmethyl)amine (TBTA) in the presence of NEt_3 in dry THF at 60 ºC. Finally, the monosilylated precursor **P1** was achieved after removal of the protecting group. In a similar manner, **P2** was efficiently synthesized by the click reaction between the alkyne **4** and the disilylated azide **7**[81] followed by deprotection (four steps, 76 % overall yield from **1**) (Scheme 1).

Scheme 1. Synthesis of the silylated precursors **P1** and **P2**.

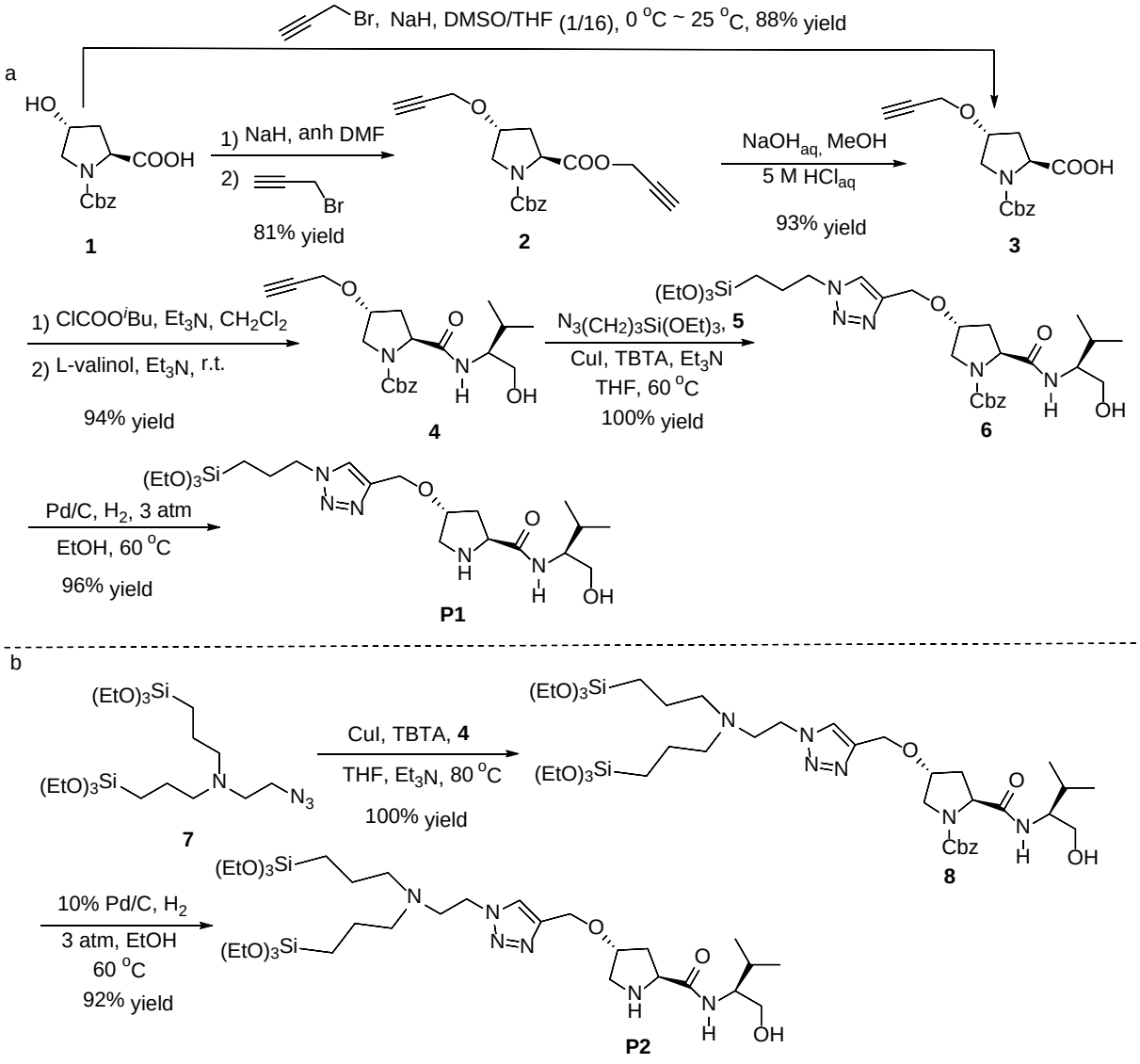

The silylated compounds **P1** and **P2** were fully characterized by ^1H and ^{13}C NMR spectroscopy. The performance of 1D and 2D NMR experiments (1D ^1H, 2D ^1H,^1H-COSY,

^{1}H,^{1}H-TOCSY, ^{1}H,^{1}H-NOESY, ^{1}H,^{13}C-HSQC and ^{1}H,^{13}C-HMBC) and the coordinated analysis of the resulting spectra allowed the complete characterization of the molecules (see details in Figure S1 and Table S1 in the Supporting Information).

We should emphasize that direct aldol reactions had been tested with homogeneous proline-valinol thioamides, which should provide better selectivities than the corresponding amides due to the higher acidity of the NH group of the thioamide relative to the NH amide functionality.[33] However, all our efforts to achieve the corresponding silylated thioamide precursors were unsuccessful. For this reason, we decided to prepare and test the nanomaterials derived from the efficiently synthesized silylated amides.

From the precursors **P1** and **P2**, six different functionalized mesoporous silica nanoparticles were prepared by sol-gel co-condensation methodology and by grafting on mesostructured silica nanoparticles of MCM-41 type[54] and **M0**.[82] The MSN of MCM-41 type were prepared[54] under basic conditions (NaOH) in the presence of a cationic template (CTAB) and showed a regular hexagonal array of uniform channels. **M0** nanoparticles were obtained[82] in a buffer solution of pH 7 with a mixture of cationic and nonionic surfactants (CTAB and Brij-56) resulting in a more disordered wormlike mesostructure (see Experimental Section and Supporting Information, Figure S2 and Figure S3). Specifically, **M1** and **M2** were synthesized by anchoring the precursors P1 and **P2**, respectively, to MCM-41 MSN under standard conditions (Scheme 2a). Similarly, **M3** and **M4** were prepared in analogous manner by grafting **P1** and **P2** to **M0** MSN, respectively (Scheme 2b). Finally, materials **M5** and **M6** were obtained by co-condensation of precursors **P1** and **P2** with tetraethyl orthosilicate (TEOS) using Brij-56 and hexadecyltrimethylammonium bromide (CTAB) as templates, in an analogous manner to **M0**. They were synthesized in an aqueous buffer solution of pH 7 from mixtures with the molar ratios Brij-56 : CTAB : TEOS : $\mathbf{P_n}$: H_2O = 1 : 20 : 160 : 16 : 120000. The final solution was

stirred at 95 ºC for 8 h (Scheme 2c) and then the nanoparticles were collected by centrifugation (13500 rpm) at room temperature. The surfactants were removed from the obtained solid by treatment with an ethanolic solution of NH_4NO_3 and then the resulting material was washed successively with ethanol, Mili-Q water and ethanol.

Scheme 2. Preparation of mesoporous organosilica nanoparticles **M1-M6.**

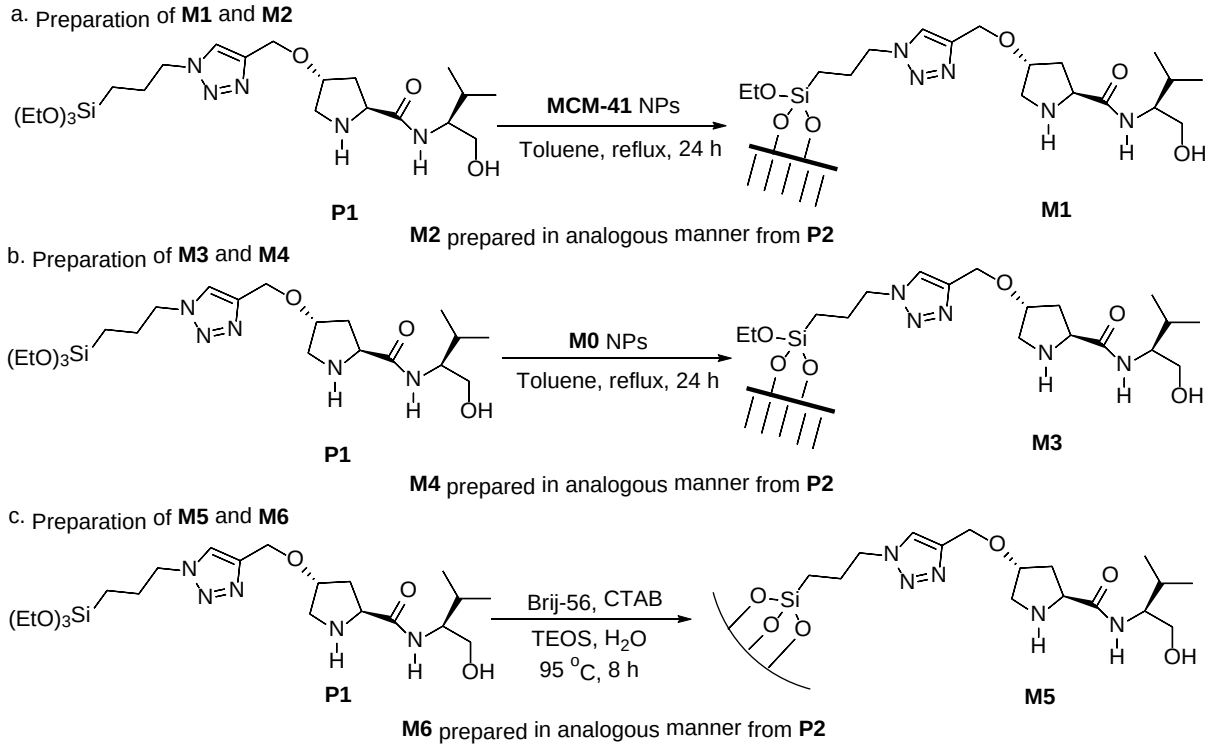

The materials were characterized by elemental analysis, ^{13}C and ^{29}Si CP MAS solid state NMR, transmission electron microscopy (TEM), scanning electron microscopy (SEM), nitrogen-sorption measurements, dynamic light scattering (DLS), zeta-potential, infrared spectroscopy (IR) and powder X-ray diffraction (p-XRD). Some physical data are given in Table 1.

Table 1. Some physical data of **M1-M6** and parent MSNs **(MCM-41** and **M0).**

Material	S_{BET} (m^2g^{-1})	V_{pore} [a] (cm^3g^{-1})	$Ø_{pore}$ [b] (nm)	Catalyst loading [c] ($mmolg^{-1}$)	Particle size (nm)		Zeta potential
					TEM	DLS[d]	
MCM-41	1097	0.79	2.7	-	100 to 600	110, 450	-25
M1	682	0.29	2.6	0.78	100 to 600	nd[e]	nd[e]
M2	477	0.21	2.5	0.69	100 to 600	80, 520	49
M0	332	0.29	3.1	-	75±8	100	-25
M3	183	0.14	3.0	0.48	84±10	250	25
M4	177	0.13	3.0	0.37	78±7	140	40
M5	135	0.09	2.5	0.82	107±10	360	20
M6	16	0.02	-	0.80	-	nd[e]	nd[e]

[a] Determined from the uptake at saturation at $p/p^o = 0.8$. [b] Determined by NLDFT. [c] Calculated from the N elemental analysis. [d] Hydrodynamic diameters. From Pade Laplace fitting. [e] Not determined (aggregated nanoparticles).

The materials were first investigated by electron microscopies, to confirm their nanosize. **M1** and **M2**, obtained from MCM-41 NPs by grafting, preserve the initial rod-like morphology with lengths from 100 to 600 nm. The TEM images display the typical parallel channels throughout the rods in all three cases. Similarly, **M3** and **M4**, obtained from **M0**, preserve the initial spherical morphology, with diameters around 80 nm. The TEM images clearly indicate the presence of pores, though they are not organized as in MCM-41. Interestingly, the synthesis of **M5** by co-condensation with 10 mol% of the elaborated organosilane **P1** yielded spherical NPs uniform in size (110 nm), with the same type of porosity as for **M0**, as seen by TEM. However, the same synthesis from the bis-silylated precursor **P2** afforded aggregated nanoobjects **M6** with no visible porosity. These results are also supported by SEM as well as

by DLS analyses (Table 1 and Supporting Information). Selected SEM and TEM images for materials **M1** and **M5** are shown in Figure 1 (see Supporting Information for TEM and SEM of other materials, Figures S4-S9).

Figure 1. SEM and TEM images of **M1** (a, b) and **M5** (c, d)

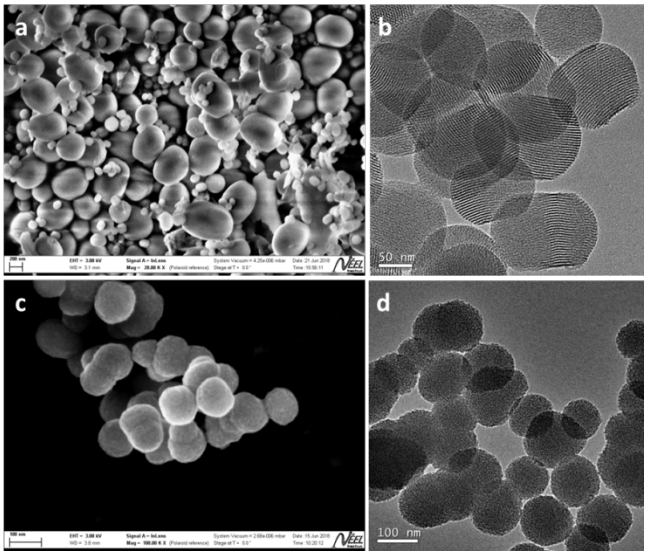

The porosity of the materials was probed by N_2-sorption experiments: for **M1** and **M2**, prepared by grafting from MCM-41, the surface area and pore volumes were significantly reduced compared to the parent MSNs whereas the pore diameter was only slightly decreased, in agreement with what is usually observed. The specific surface areas and pore volumes for the **M0**-derived materials **M3** and **M4** are significantly lower (surface areas from 330 to 180 m^2/g after grafting, and 135 m^2/g for **M5** obtained by co-condensation, Table 1). Except for **M6**, which is not porous, all materials display isotherms typical of mesoporous materials with small pores (no hysteresis) (Figure 2). Indeed, the pore diameters of all these materials lie in the range 2.5-3.0 nm. The contribution of micropores is negligible for all materials except **M5**, which displays ca 40 m^2/g of microporous surface area. The p-XRD analyses (see Supporting Information) only showed an organized porosity for the MCM-41-derived materials **M1** and

M2, typical for a hexagonal 2D symmetry with a sharp Bragg peak (1,0) and the two first harmonics ((1,1) and (2,0)). The broad pattern observed for **M0** and related materials (**M3** and **M4** from grafting and **M5** from co-condensation) is typical for porous materials with no organization of pores, and is even not detected for **M6**, which is in agreement with its very low porosity.

Figure 2. N_2-sorption isotherms of **M1-M6.**

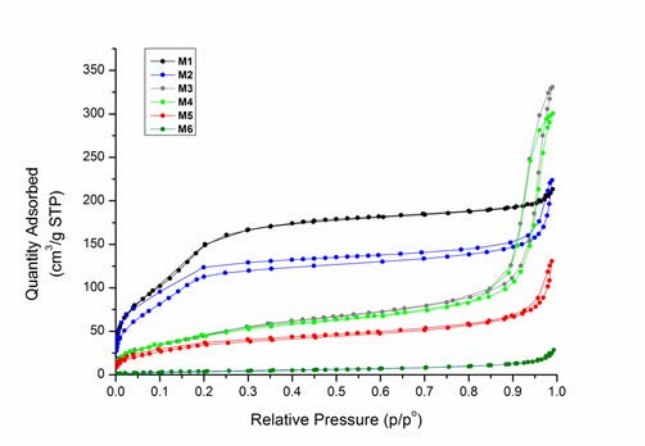

The presence of the organic ligand in the nanomaterials was ensured by the solid-state NMR spectra (^{29}Si and ^{13}C). The ^{29}Si CP MAS NMR spectra (**M1**, **M3**, **M5**, **M6**) showed two groups of chemical shifts: T units from -59 to -69 ppm resulting from the organosilanes **P1**, and Q units ranging from -93 to -113 ppm formed from TEOS, as exemplified by the ^{29}Si CP MAS NMR spectrum of **M1** and **M5** (Figure 3 bottom). Indeed, the presence of T signals suggested that the integrity of the Si-C bond was maintained during the formation of the nanomaterial, which was also confirmed by the ^{13}C solid state NMR spectrum with the strong signal at 8 ppm (Figure 3 top). The superposition of the ^{13}C spectra of **P1** in solution and of **M5** shows a good similarity between the two spectra, suggesting thereby the integrity of the organic skeleton. For both **M1** (grafting) and **M5** (co-condensation) the ^{29}Si NMR display mostly T2 (-58 ppm) and

T3 (-67 ppm) environments, which confirms the strong anchoring of the organic frameworks within the silica network by two or three Si-O-Si linkages.

Figure 3. ^{13}C NMR spectra of **M5** and **P1** (top) and ^{29}Si CP MAS spectra of **M1** and **M5** (bottom).

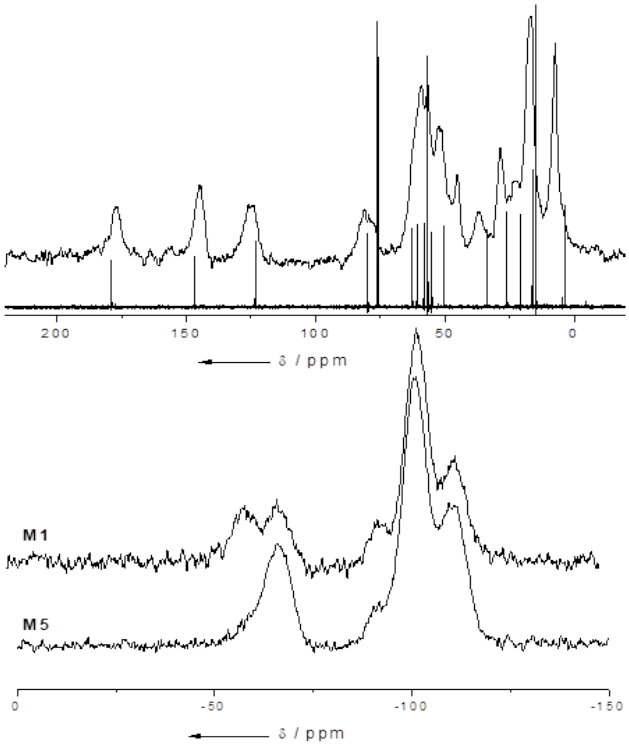

The catalyst loading was inferred from the nitrogen elemental analysis (Table 1), with **M5** presenting the highest loading (0.82 mmol g^{-1}). Finally, the dispersibility of the NPs was checked in dilute NaCl aqueous solution. Except for **M1** that was not easily dispersible, the NPs were moderately aggregated after dispersion at 1 mg/mL. The zeta potential ζ evolved from ca -25 mV at pH 7 for the pure silica samples MCM-41 and **M0**, in agreement with an isoelectric point of ca 3.5 for silica, to positive values for the functional materials which display amino groups that are protonated at pH 7. Indeed, the ζ potential was *ca* +25 mV when

precursor **P1** was grafted or co-condensed and *ca* +45 mV when precursor **P2** was employed. This agrees with the higher density in amino groups in materials derived from **P2** (two amino groups in its structure) compared to **P1** (one amino group), which results in more protons attached to the surface of the NPs at neutral pH.

It is worth to mention that **M5** is the first nanosized chiral organocatalyst obtained by co-condensation procedures.

Catalytic activity and recyclability of M1-M6 in direct asymmetric aldol reaction

The activity of the functionalized mesoporous nanoparticles was then evaluated via a typically used benchmark reaction for the direct asymmetric aldolisations, the reaction between p-nitrobenzaldehyde **9a** and cyclohexanone **10a** to give aldol **11aa** as a diastereomeric mixture. We first undertook a screening of reaction conditions (catalytic nanomaterial, solvent, temperature, reaction time) using a 10 mol% of catalyst, an excess of ketone and a 2 M concentration of aldehyde, as summarized in Table 2. Initial experiments performed with **M1** in water at room temperature and at 0 ºC gave full conversion in 6 and 8 h, respectively (entries 1 and 2 of Table 2). Thus, lower temperature resulted in a slight decrease of the reaction rate, but the selectivity was improved up to an anti/syn ratio of 89/11 and an enantiomeric ratio (er) for the major anti isomer of 91/9. We next examined the effect of solvent with the same catalyst **M1** and an initial temperature of 0 ºC. We observed a very significant decrease in the conversion and selectivity with the use of tetrahydrofuran, acetonitrile, ethyl acetate, toluene, dimethylformamide and dimethylsulfoxide (entries 3-8 of Table 2). The reaction performed in brine at 0 ºC (entry 9 of Table 2) gave a selectivity similar to that of entry 2, but the reaction was much slower than in distilled water. Under neat conditions at the same temperature, a clear deleterious effect was found in both the reactivity and asymmetric induction (entry 10 of Table 2). The catalytic tests with the other nanoparticles **M2-M6** were then performed with a 10

mol% loading in water at 0 ºC (entries 11-15 of Table 2). The best result was obtained with **M5**, for which a full conversion was achieved after 11 h (dr 89/11, er_{anti} 92/8, entry 14 of Table 2). The next step was to determine the influence of the catalyst loading on the aldol reaction with **M5** in water at 0 ºC (5 and 15 mol%, entries 16-17 of Table 2 compared with 10 mol% of entry 14). Whereas the reaction rate was affected as expected, the diastereo- and enantioselectivity did not change significantly. Finally, we have found that the addition of 10% of benzoic acid as co-catalyst to **M5** and **M1** slightly improves the enantioselectivity, but has a deleterious effect on the reaction rate (compare entries 18 and 19 with entries 14 and 2 in Table 2). In any case, it appears that the materials derived from the monosilylated precursor **P1** showed better performance than those derived from the disilylated **P2.** The two points of attachment of the catalytic moiety to the matrix in the case of materials **M2**, **M4** and **M6** probably induce less flexibility to this moiety, limiting the right approach to the reactants for an optimal activity and selectivity.

As mentioned before, the use of organosilica nanoparticles should reduce the problems of diffusion and low reaction rates encountered with bulk organosilicas. The reaction times required for complete conversion in this aldol reaction with **M1** and **M5** compete well with those found for an homogeneous proline-valinol thioamide (5 mol% cat, 10 mol% PhCOOH, water, 0 ºC to rt, 8 h, 94% yield),[33] with the added advantage over the homogeneous organocatalyst that there is no need of acid co-catalyst in our experiments to accelerate the reaction. Moreover, faster reaction rates are observed here than with silica-supported prolinamides (10 mol% cat, water, 7-24 h at rt for 99% conversion, and 6 d at 5ºC for 80% conversion)[74] and prolinsulphonamides (10 mol% cat, water, rt, 4 d for 99% conversion).[75]

Table 2. Screening of the reaction conditions for asymmetric aldol reaction between p-nitrobenzaldehyde **9a** and cyclohexanone **10a**.

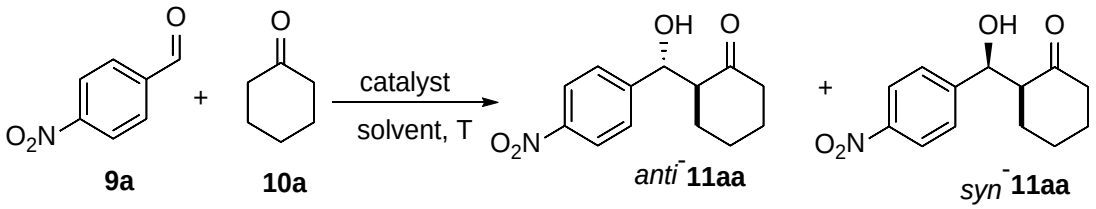

Entry[a]	**M**	Solvent	T (°C)[b]	t (h)	Yield (%)[c]	$dr_{anti/syn}$[d]	er_{anti}[e]
1	**M1**	H_2O	rt	6	> 99	86/14	88/12
2	**M1**	H_2O	0	8	> 99	89/11	91/9
3	**M1**	THF	0 - rt	24	16	75/25	61/39
4	**M1**	CH_3CN	0 - rt	24	39	87/13	88/12
5	**M1**	EtOAc	0 - rt	52	80	83/17	70/30
6	**M1**	toluene	0 - rt	52	60	85/15	77/23
7	**M1**	DMF	0 - rt	64	19	78/22	80/20
8	**M1**	DMSO	0 - rt	96	31	70/30	78/22
9	**M1**	brine	0	31	> 99	87/13	91/9
10	**M1**	neat	0	24	49	83/17	54/46
11	**M2**	H_2O	0	24	> 99	85/15	89/11
12	**M3**	H_2O	0	16	> 99	85/15	81/19
13	**M4**	H_2O	0	26	90	87/13	82/18
14	**M5**	H_2O	0	11	> 99	89/11	92/8
15	**M6**	H_2O	0	48	> 99	84/16	88/12
16[f]	**M5**	H_2O	0	26	> 99	90/10	93/7
17[g]	**M5**	H_2O	0	8	> 99	89/11	91/9
18[h]	**M5**	H_2O	0	22	> 99	88/12	95/5
19[h]	**M1**	H_2O	0	29	> 99	86/14	96/4

[a] Molar ratio **9a**/**10a**/**M** = 10:50:1; 0.5 mL of solvent per mmol of **9a**. [b] 0 - rt means the first 12 h at 0 ºC and then at room temperature. [c] Isolated yield of the diastereomeric mixture. [d] Determined by ^{1}H NMR spectroscopy. [e] Enantiomeric ratio determined by chiral HPLC (Daicel Chiralpak AD-H column). [f] Molar ratio **9a**/**10a**/**M** = 20:100:1. [g] Molar ratio **9a**/**10a**/**M** = 20:100:3. [h] Benzoic acid was added (10 mol%) as co-catalyst.

After the optimization stage, we investigated the reusability of **M1** (10 mol%) in the same aldol reaction between **9a** and **10a** performed in water at 0 ºC for 8 h (conditions of entry 2 in Table 2). The recycling procedure consisted in the addition of ethyl acetate to the crude mixture, centrifugation to separate the nanoparticles and decantation of the supernatant to isolate the product. To our delight, we found that the activity, diastereo- and enantioselectivity were maintained up to five consecutive cycles (Table 3).

Table 3. Recycling of **M1** in the asymmetric aldol reaction between *p*-nitrobenzaldehyde **9a** and cyclohexanone **10a** in water**.**

Cycle [a]	Yield (%)[b]	$dr_{anti/syn}$ [c]	er_{anti} [d]
1	> 99	89/11	91/9
2	> 99	88/12	89/11
3	> 99	89/11	90/10
4	> 99	89/11	91/9
5	> 99	89/11	91/9

[a] Molar ratio **9a**/**10a**/**M5** = 10:50:1; 0.5 mL of water per mmol of **9a**, 0 ºC, 8 h. [b] Isolated yield of the diastereomeric mixture of **11aa**. [c] Determined by ^{1}H NMR spectroscopy. [d] Enantiomeric ratio determined by chiral HPLC (Daicel Chiralpak AD-H column).

No significant changes between fresh and reused **M1** were found by comparison of *p*-XRD (Figure S10 in Supporting Information), TEM (Figure S11 in Supporting Information), FT-IR (Figure S12) and elemental analysis (the initial amount of catalyst of 0.8 mmol g^{-1} was maintained after the 5th cycle). Moreover, the reusability has also been successfully proved with **M5** (see Figures S13-S16 in Supporting Information).

On the basis of the optimal conditions, we chose **M1** and **M5** as the best catalysts to examine the scope of the aldol reaction of cyclohexanone **10a** with a variety of aromatic aldehydes **9a-i** (Table 4) in water, at 0 ºC, with an amount of catalyst of 10 mol%, in the absence of any co-catalyst (conditions of entries 2 and 14, Table 2). Also, **M3** was considered as catalyst for extending the scope. The corresponding aldol products were obtained in high isolated yields (71 to >99 %) with good to excellent anti/syn diastereoselectivity (*dr* from 81/19 to 90/10) and enantioselectivity for the major anti isomer (*er* from 81/19 to 95/5) (entries 1-25, Table 4). The reaction with *p*-nitrobenzaldehyde **9a** provided the highest reaction rates (entries 1-3, table 4). Lower reactivity was found for *o*-nitrobenzaldehyde **9b** (entries 4-6, Table 4) and 2,4-dinitrobenzaldehyde **9c** (entries 7-9, Table 4), probably due to steric hindrance of the *ortho*-substituent. The selectivity was also good for aldehydes bearing halogeno groups in *para* and/or *ortho* position (entries 10-21 in Table 4). Curiously, 2-chlorobenzaldehyde **9g** provided higher yields than 4-chlorobenzaldehyde **9d** (compare entries 16-17 with entries 10-11 in Table 4). Also *p*-trifluoromethylbenzaldehyde **9i** furnished excellent yields and selectivities with all the tested catalysts (entries 22-24 in Table 4). The aldol reaction of **9a** was then successfully extended to the ketone **10b** (entries 25-27 in Table 4). The order of the performance of the materials would be **M1** > **M5** > **M3** with respect to the reaction rates, although we have observed differences on this order depending on the substrate. We should also consider that the reaction times were not optimized in all cases (control was not performed during the night). Regarding the selectivity, the order would be **M5** > **M1** ≥ **M3**, but sometimes the differences in the selectivity were not very significative. Curiously, whereas **M3** gave lower *dr* and *er* for **11aa** (entry 3, Table 4), the enantioselectivities with this catalyst were improved for other substrates (entries 6, 9, 18, 21, 24, 27 of Table 4). Taking all that into account, a simple rationalization of the different performances of the materials does not seem feasible.

Table 4. Direct asymmetric aldol reactions between aromatic aldehydes **9** and ketones **10** to give aldols **11** with **M1**, **M3** and **M5**

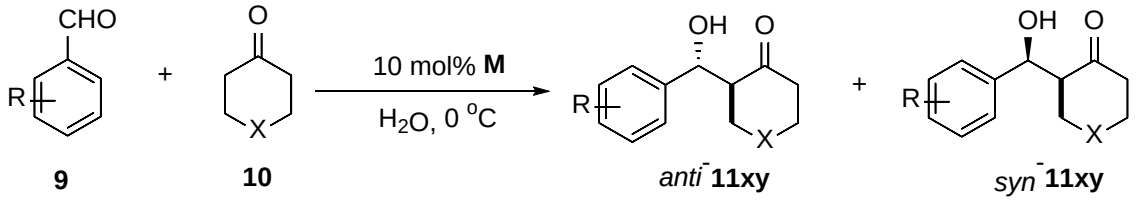

9 **10** *anti*-**11xy** *syn*-**11xy**

x = a, b ; y = a-i

9a: R = 4-NO_2 **9f**: R = 4-Br **10a**: X = CH_2
9b: R = 2-NO_2 **9g**: R = 2-Cl **10b**: X = O
9c: R = 2,4-NO_2 **9h**: R = 2,4-Cl
9d: R = 4-Cl **9i**: R = 4-CF_3
9e: R = 4-F

Entry[a]	9	10	11xy[b]	M	t (h)	Yield (%)[c]	$dr_{anti/syn}$ [d]	er_{anti} [e]
1	**9a**	**10a**	**11aa**	**M1**	8	> 99	89/11	91/9
2	**9a**	**10a**	**11aa**	**M5**	11	> 99	89/11	92/8
3	**9a**	**10a**	**11aa**	**M3**	14	> 99	85/15	81/19
4	**9b**	**10a**	**11ab**	**M1**	25	96	90/10	92/8
5	**9b**	**10a**	**11ab**	**M5**	30	97	90/10	94/6
6	**9b**	**10a**	**11ab**	**M3**	26	97	87/13	89/11
7	**9c**	**10a**	**11ac**	**M1**	54	94	86/14	90/10
8	**9c**	**10a**	**11ac**	**M5**	52	94	87/13	93/7
9	**9c**	**10a**	**11ac**	**M3**	56	94	87/13	89/11
10	**9d**	**10a**	**11ad**	**M1**	54	76	87/13	87/13
11	**9d**	**10a**	**11ad**	**M5**	80	71	86/14	95/5
12	**9e**	**10a**	**11ae**	**M1**	30	81	86/14	91/9
13	**9e**	**10a**	**11ae**	**M5**	48	75	87/13	92/8
14	**9f**	**10a**	**11af**	**M1**	48	97	90/10	92/8
15	**9f**	**10a**	**11af**	**M5**	48	89	87/13	93/7
16	**9g**	**10a**	**11ag**	**M1**	24	97	85/15	93/7
17	**9g**	**10a**	**11ag**	**M5**	22	96	88/12	94/6
18	**9g**	**10a**	**11ag**	**M3**	26	95	87/13	91/9

19	**9h**	**10a**	**11ah**	**M1**	24	97	81/19	92/8
20	**9h**	**10a**	**11ah**	**M5**	24	98	84/16	95/5
21	**9h**	**10a**	**11ah**	**M3**	30	95	83/17	91/9
22	**9i**	**10a**	**11ai**	**M1**	22	> 99	88/12	91/9
23	**9i**	**10a**	**11ai**	**M5**	28	> 99	89/11	94/6
24	**9i**	**10a**	**11ai**	**M3**	36	> 99	84/16	91/9
25	**9a**	**10b**	**11ba**	**M1**	9	> 99	88/12	90/10
26	**9a**	**10b**	**11ba**	**M5**	12	> 99	89/11	95/5
27	**9a**	**10b**	**11ba**	**M3**	10	> 99	90/10	93/7

[a] Molar ratio **9**/**10**/**M** = 10:50:1; water, 0 ºC; 0.5 mL of water/mmol of **9**. [b] In the numbering of **11xy**, **x** refers to the starting ketone and **y** to the starting aldehyde. [c] Isolated yield. [d] Determined by ^{1}H NMR spectroscopy. [e] Enantiomeric ratio determined by chiral HPLC (Daicel Chiralpak AD-H and OD-H columns).

After the scope investigation, the variation of yield, diastereo- and enantioselectivity with the reaction time has been studied for the reaction between **9a** and **10a** with **M1** as catalyst in water at 0 ºC (conditions of entry 1, Table 4) (see Figure S17 (a) in Supporting Information). Along the reaction time, the yield of **11aa** exhibited a Langmuir type increase,[44] reaching almost the maximum at 7 h. The *dr* remained constant after 3 h of reaction and the *ee* holded almost the same values along the time. A pseudo-first order kinetics plot was found (see Figure S17 (b) in Supporting Information) by following the variation of the concentration of limiting aldehyde **9a** along the reaction time,[83] with an observed rate constant of 0.48 ± 0.02 h $^{-1}$.

This reaction has not been carried out with the analogous homogeneous proline-valinol amide, but with the homogeneous proline-valinol thioamide.[33] As previously mentioned, the authors found better performances for thioamides due to the higher acidity of the NH group of thioamide relative to the NH of the amide. In order to compare the heterogeneous catalyst **M1** with the homogeneous proline-valinol amide, we conducted the aldol reaction between *p*-nitrobenzaldehyde **9a** and acetone (5 equiv) in water at 0 ºC (10 mol% of **M1**) to give the corresponding aldol product in quantitative yield after 10 h with an *ee* of 46%. In the case of

the homogeneous proline-valinol amide[33] the same reaction was not performed in water, but in DMSO at 0 ºC (10 mol% of catalyst) furnishing the aldol product in only 43% yield after 12 h with an *ee* of 55%. Thus, our catalyst in aqueous conditions reacts faster than the homogeneous one in dimethylsulfoxide, and the enantioselectivity remains moderate in both cases.

For a better comparison between the performances of homogeneous and heterogeneous catalysts, the reaction between **9a** and **10a** (entry 1 of Table 4) was also carried out with the monosilylated precursor **P1**, in spite of the risk of a slow hydrolysis of the triethoxysilyl group in water. In the absence of acid co-catalyst a reaction time between 12 and 24 h was needed for complete conversion (no control was performed during the night) to obtain the diastereomeric mixture **11aa** with lower selectivity (*dr* = 76/24; er_{anti} = 79/21) than with the heterogeneous catalyst **M1**. The reaction rate and enantioselectivity of **P1** were improved by the addition of benzoic acid to achieve the same values as with **M1**, although the diastereoselectivity was somewhat lower (reaction time = 8 h, *dr* = 82/18, er_{anti} = 91/9).

As previously pointed out, the proposed mechanism for the aldol reaction with the proline-valinol amides and thioamides is based on the proline catalysis concept and double hydrogen bonding activation of the electrophilic aldehyde (by the NH and the OH groups).[33] The reaction begins with the condensation of the cyclohexanone with the amine fragment of the proline derived organocatalyst to form a nucleophilic enamine, which would attack the aldehyde to give, after hydrolysis, the desired aldol product.[42] The enantioselection would arise from the positioning of the aldehyde via the double hydrogen bonding through the NH and OH groups of the proline-valinol amide moiety. From the previously mentioned experiments, it is clear that the reaction with the heterogeneous catalyst benefits from the acidic silanol groups on the surface of the organosilica nanoparticles, which play the role of co-catalyst. However, the Si-OH groups might also have a deleterious effect on the selectivity, competing with the NH and/or OH groups of the organocatalyst for the positioning of the aldehyde. In view of the

comparison between **P1** and **M1**, this interference does not seem to be very important in our case, but might modulate the selectivity depending on the material and the substrate.

These results proved that we have developed robust nanocatalytic systems, which can be applied to a variety of substrates. We should emphasize that the developed procedure is very simple and environmentally friendly (aqueous medium, 0 ºC, no acid co-catalyst, relatively low loadings of the nanocatalyst, easy separation and recycling of the catalyst).

CONCLUSIONS

In summary, we have prepared mesoporous organosilica nanoparticles derived from mono- and bis-silylated proline-valinol amides **P1** and **P2**. The action of these dipeptide derivatives relies on the proline catalysis concept (enamine pathway) and double hydrogen bonding activation. The linking between the organocatalytic moiety and the silylated group was build through a copper-catalyzed azide-alkyne cycloaddition reaction (CuAAC) under anhydrous conditions. For the preparation of the nanomaterials, we have used both a grafting procedure to previously synthesized mesoporous silica nanoparticles (MSN) and a co-condensation method with TEOS in a buffered neutral medium with Brij-56/CTAB as templates. *For the best of our knowledge, this is the first report on the obtention of functionalized mesoporous silica nanoparticles by co-condensation procedures with a chiral precursor of a certain structural complexity*. The functionalized mesoporous silica nanoparticles **M1-M6** have been fully characterized by elemental analysis, ^{29}Si and ^{13}C CP MAS NMR spectroscopy, TEM, SEM, N_2-sorption measurements, DLS, zeta-potential, IR and p-XRD. We have then evaluated their activity and recyclability as catalysts in the asymmetric aldol reaction between several aromatic aldehydes **9a-i** and ketones **10a-b** to afford efficiently aldols **11** as an *anti/syn* diastereomeric mixture with good diastereo- and enantiomeric ratios (up to dr 90/10 and er 96/4). The best catalysts were **M1** derived from grafting of the monosilylated **P1** to MSN of MCM-41 type and **M5** synthesized from **P1** by co-condensation (TEOS:**P1**=10:1). The

optimized protocol for the organocatalyzed aldol reaction is simple and environmentally friendly. The reaction takes place in water at 0 ºC, no acid co-catalyst is needed, relatively low loadings of the nanocatalyst (5-10 mol%) are required, the catalyst is easily recovered by centrifugation and decantation, avoiding chromatographic separation. ***M1** has been recycled up to five runs with no loss of activity and selectivity*. The use of organosilica nanoparticles decreases the problems of diffusion and low reaction rates encountered with bulk organosilicas. *For the best of our knowledge, this is the first report of asymmetric induction on the direct aldol reaction achieved by mesoporous silica nanoparticles derived chiral organocatalysts.*

EXPERIMENTAL SECTION

General information

The ^{1}H and ^{13}C NMR spectra in solution were recorded on Bruker DPX-360 or Bruker Avance-II 600 spectrometers, operating at ^{1}H NMR frequencies of 360.13 and 600.13 MHz respectively, and at 298.0 K of temperature. 1D ^{1}H and 2D ^{1}H,^{1}H-COSY, ^{1}H,^{1}H-TOCSY, ^{1}H,^{1}H-NOESY, ^{1}H,^{13}C-HSQC, and ^{1}H,^{13}C-HMBC experiments were performed using standard Bruker pulse sequences and acquired under routine conditions. All the spectra were calibrated using the residual solvent signal ($CHCl_3$, δ_H, 7.26 and δ_C, 77.16 ppm). Chemical shift data were expressed in ppm and coupling constant (*J*) values in Hz. Multiplicity of peaks was abbreviated as s (singlet), d (doublet), t (triplet), q (quartet) and dd (doublet of doublets). The ^{29}Si and ^{13}C CP-MAS NMR spectra were obtained from a Bruker AV400WB, the repetition time was 5 seconds with contact times of 5 milliseconds. These NMR instruments belong to the *Servei de Ressonància Magnètica Nuclear* of the *Universitat Autònoma de Barcelona* (UAB). From the *Servei d'Anàlisi Química* of the *Universitat Autònoma de Barcelona* the following experimental data were acquired: infra-red spectra (IR), specific rotation ($[\alpha]_D$), mass-spectrometry (MS) and elemental analysis (EA). IR spectroscopy was recorded with a Bruker Tensor 27 spectrometer using a Golden Gate ATR module with a diamond window. Specific

rotation values were obtained at 20 ºC in a JASCO J-175 polarimeter at 589.6 nm and they are given in 10^{-1} deg cm^2 g^{-1}. Low- and high-resolution mass spectra were obtained by direct injection of the sample with electrospray techniques in a Hewlett-Packard 5989A and *microTOF-Q* instruments respectively. Elemental analysis of C, N and H were performed using Flash 2000 Organic Elemental analyser of Thermo Fisher Scientific with BBOT as an internal standard. Transmission Electron Microscopy (TEM) analyses were performed in the *Servei de Microscòpia* of UAB on a JEM-2011 Electron Microscope 200 Kv. Powder X-ray diffraction (p-XRD) was performed in the *Servei de Difracció de Raigs X* of UAB with X'Pert Power from PANalytical 45Kv/40 mA, K_α 1.5419 Å with a cooper anode. Field Effect Scanning Electron Microscopy (FESEM), Dynamic light scattering (DLS) and Zeta potential were obtained from the Institut Néel. FESEM images were obtained with a Zeiss Ultra+ scanning electron microscope. The NPs in powder form were deposited on doped silicon wafers with carbon tape for observation without metallization. A voltage of 3 kV was used at a working distance of 3 mm. DLS analyses were performed using a Vasco Kin instrument from Cordouan Technologies. Zeta potential measurements were performed on a Wallis instrument from Cordouan Technologies. The enantiomeric ratio (*er*) of the products was determined by chiral stationary phase HPLC (chiral columns Daicel Chiralpak AD-H and OD-H) with a Waters 2960 instrument using a UV photodiode array detector in our group. The surface areas were determined by the Brunauer-Emmet-Teller (BET) method from N_2 adsorption-desorption isotherms obtained with a Micromeritics ASAP2000 analyzer which belongs to *Institut de Ciència dels Materials de Barcelona (ICMAB)* after degassing samples for 30 h at 55 °C under vacuum. The pore diameter distribution was calculated by Non-Local Density Functional Theory (NLDFT) method in model: N_2@77 K on Carbon Slit Pores. When required, experiments were carried out with standard high vacuum and Schlenk techniques. Chromatographic purifications were performed under N_2 pressure using 230-400 mesh silica

gel (flash chromatography). Dry toluene was purchased from Merck. Dry solvents and reagents were obtained following standard procedures: triethylamine was distilled over CaH_2; CH_3CN was dried by molecular sieves, THF and pentane were from solvent processing equipment (*PureSolv*, Innovative Technology).

Although the organic azides used in this work are stable and not harmful, appropriate precautions should always be taken when manipulating azides. Silylated azides **5**[84] and **7**[81] were prepared according to the literature.

*Synthesis of (2S,4R)-1-((benzyloxy)carbonyl)-4-(prop-2-yn-1-yloxy)pyrrolidine-2-carboxylic acid, **3**.* To a flame-dried three-necked round bottom flask was placed NaH (3.12 g of 60% in mineral oil, corresponding to 1.87 g of NaH, 78.0 mmol) under N_2, then the flask was cooled to 0 °C and a solution of **1** (8.04 g, 30.0 mmol) in a mixture of anhydrous THF (62 mL) and DMSO (5.0 mL) was slowly added by syringe. The heterogeneous mixture was stirred for 30 min at 0ºC. Then, a solution of propargyl bromide (11.15 g of 80 wt. % in xylene, corresponding to 8.92 g of propargyl bromide, 75.0 mmol) in THF (18.0 mL) was added by syringe. The reaction mixture was stirred at room temperature until **1** was completely consumed (TLC monitoring, 18 h). The reaction was then quenched with water (60.0 mL) and the pH was adjusted to 4 with 10% aqueous solution of $KHSO_4$. The crude solution was extracted with AcOEt (3 × 120 mL). The organic layer was washed with brine (3 × 60 mL), dried over Na_2SO_4, and the solvent was evaporated under vacuum. The acid **3**[77] was isolated by flash column chromatography on silica gel with EtOAc/MeOH = 9:1 to afford colorless oil (8.01 g, 88 % yield). $[\alpha]_D^{20}$ = -66 º (C 0.01, CH_2Cl_2). ^{1}H NMR (360 MHz, $CDCl_3$) (mixture of rotamers) δ 10.96 (s, 1H), 7.36-7.24 (m, 5H), 5.20-5.07 (m, 2H), 4.52-4.44 (m, 1H), 4.34-4.33 (m, 1H), 4.20-4.08 (m, 2H), 3.79-3.61 (m, 2H), 2.50-2.38 (m, 2H), 2.26-2.14 (m, 1H). ^{13}C NMR (91 MHz, $CDCl_3$) (mixture of rotamers) δ 177.7, 176.5, 155.6, 154.5, 136.2, 136.1,

128.4, 128.2, 127.99, 127.64, 79.14, 79.12, 76.2, 75.6, 75.2, 67.7, 67.4, 57.99, 57.54, 56.48, 56.45, 51.69, 51.62, 36.6, 35.1.

Synthesis of benzyl (2S,4R)-2-(((S)-1-hydroxy-3-methylbutan-2-yl)carbamoyl)-4-(prop-2-yn-1-yloxy)pyrrolidine-1-carboxylate, ***4***. To a stirred solution of **3** (7.58 g, 25.0 mmol) in CH_2Cl_2 (20 mL), Et_3N (5.20 mL, d = 0.73 g/mL, 37.5 mmol) was slowly added at 0 °C. After the solution had been stirred for 10 min, isobutyl chloroformate (3.93 g, 28.75 mmol) was added dropwise at 0 °C. After the reaction mixture had been stirred for additional 20 min at 0 °C, a solution of Et_3N (3.99 mL, d = 0.73 g/mL, 28.75 mmol) and L-valinol (2.97 g, 28.75 mmol) in CH_2Cl_2 (10 mL) was added. The reaction mixture was then warmed up to room temperature and it was stirred at room temperature overnight. The reaction was quenched by addition of 1M HCl and diluted with CH_2Cl_2 (80 mL), the organic phase was washed with H_2O (3 × 30 mL), brine (2 × 30 mL) and dried over anhydrous Na_2SO_4, filtered, and then concentrated under reduced pressure. Recrystallization of the residue (CH_2Cl_2/hexane) gave **4** as a white solid (9.12 g, 94% yield). $[\alpha]D^{20}$ = -70 ^{o} (c 0.01, CH_2Cl_2). ^{1}H NMR (360 MHz, $CDCl_3$) (mixture of rotamers) δ 7.34-7.31 (m, 5H), 6.81 (s, 1H), 5.19-5.10 (m, 2H), 4.46-4.36 (m, 2H), 4.14 (s, 2H), 3.91-3.43 (m, 5H), 2.84 (s, 1H), 2.49-2.43 (m, 2H), 2.21-2.11 (m, 1H), 1.88-1.69 (m, 1H), 0.89-0.79 (m, 6H); ^{13}C NMR (91 MHz, $CDCl_3$) (mixture of rotamers) δ 171.9, 156.3, 136.1, 128.6, 126.3, 127.9, 79.3, 76.6, 74.9, 63.9, 59.5, 57.7, 56.5, 51.8, 33.9, 28.9, 19.5, 18.5. IR (film) 3415.4, 3256.6, 2958.3, 1649.9, 1556.7, 1427.5, 1176.5, 1073.6, 943.1, 811.2, 645.4 cm^{-1}. MS (ESI) m/z: 411.2, 390.2, 389.2, 371.2, 345.2, 214.1; HRMS (ESI) m/z $[M + Na]^+$ calcd for $C_{21}H_{28}N_2O_5Na$: 411.1890, found: 411.1898.

Synthesis of benzyl (2S,4R)-2-(((S)-1-hydroxy-3-methylbutan-2-yl)carbamoyl)-4-((1-(3-(triethoxysilyl)propyl)-1H-1,2,3-triazol-4-yl)methoxy)pyrrolidine-1-carboxylate, ***6***. To a dry Schlenk flask equipped with a stir bar and under nitrogen atmosphere, CuI (11.4 mg, 0.06 mmol), TBTA (31.9 mg, 0.06 mmol) and anhydrous THF (30 mL) were added. The resulting

mixture was stirred for 30 min, then **4** (1.17 g, 3.0 mmol), **5** (741 mg, 3.0 mmol) and anhydrous Et_3N (1.5 mL, 0.73 g/mL, 10.8 mmol) were added by using a syringe. The resulting mixture was stirred at 60 ºC (N_2 atmosphere) until **4** was fully consumed (14 h, TLC monitoring). Then, the solvent was evaporated under reduced pressure and the residue was washed with anhydrous pentane to provide **6** as colorless oil (1.90 g, 100 % yield). $[\alpha]_D^{20}$ = -48 º (*c* 0.01, CH_2Cl_2). ^{1}H NMR (600 MHz, $CDCl_3$) (mixture of rotamers) δ 7.51 (s, 1H), 7.34-7.27 (m, 5H), 6.78 (s, 1H), 5.29-5.12 (m, 2H), 4.63-4.59 (m, 2H), 4.54 (br s, 1H), 4.34-4.30 (m, 3H), 3.82 (q, *J* = 6 Hz, 6H), 3.74-3.58 (m, 5H), 2.45 (br s, 1H), 2.24(br s, 1H), 2.04-1.99 (m, 2H), 1.88-1.72 (m, 1H), 1.21 (t, *J* = 6 Hz, 9H), 0.89-0.79 (m, 6H), 0.62-0.59 (m, 2H), NH and OH were not detected; ^{13}C NMR (151 MHz, $CDCl_3$) (mixture of rotamers) δ 171.9, 156.4, 144.5, 136.3, 128.6, 128.3, 128.0, 122.6, 76.4, 67.6, 63.8, 62.8, 59.7, 58.6, 57.7, 52.6, 34.3, 29.0, 24.3, 22.4, 19.6, 18.4, 14.1, 7.6. IR (film) 3307, 2971, 1685, 1416, 1353, 1073, 955, 768, 697 cm^{-1}. MS (ESI) m/z: 658.3 $[M + Na]^+$, 637.3, 636.3 $[M + H]^+$, 590.3, 553.3, 531.3, 413.3, 301.1, 148.9; HRMS (ESI) m/z $[M + Na]^+$ calcd for $C_{30}H_{49}N_5O_8SiNa$: 658.3243, found: 658.3231.

Synthesis of (2S,4R)-N-((S)-1-hydroxy-3-methylbutan-2-yl)-4-((1-(3-(triethoxysilyl)propyl)-1H-1,2,3-triazol-4-yl)methoxy)pyrrolidine-2-carboxamide, ***P1*****.** A mixture of **6** (1.27 g, 2.0 mmol) and 426 mg of 10% Pd/C (0.4 mmol Pd, 20 mol%) in absolute ethanol (20 mL) was hydrogenated at 50 ºC under 3 atm of H_2 for 6 h. The mixture was filtered through Celite® 545, and the solvent from filtrate was evaporated at reduced pressure to afford **P1** as a colorless oil (962 mg, 96% yield). $[\alpha]_D^{20}$ = -26 º (*c* 0.01, CH_2Cl_2). ^{1}H NMR (600 MHz, $CDCl_3$) δ 7.88 (d, *J* = 7.2 Hz, 1H), 7.50 (s, 1H), 4.55 (d, *J* = 12.1 Hz, 1H), 4.53 (d, *J* = 12.1 Hz, 1H), 4.31 (t, *J* = 7.0 Hz, 2H), 4.12 (br s, 1H), 3.91 (t, *J* = 8.0 Hz, 1H), 3.78 (q, *J* = 7.0 Hz, 6H), 3.66-3.61 (m, 3H), 3.18 (d, *J* = 12.7 Hz, 1H), 2.70 (dd, *J* = 12.7 and 3.4 Hz, 1H), 2.38 (m, 1H), 1.99 (m, 2H), 1.90 (m, 1H), 1.88 (m, 1H), 1.18 (t, *J* = 7.0 Hz, 9H), 0.91 (d, *J* = 6.8 Hz, 3H), 0.87 (d, *J* = 6.8 Hz, 3H), 0.57 (m, 2H), NH and OH were not detected; ^{13}C NMR (151 MHz, $CDCl_3$) δ 175.5,

144.7, 122.3, 80.7, 64.2, 62.1, 59.9, 58.8, 56.9, 52.4, 52.4, 36.5, 29.0, 24.1, 19.7, 18.4, 18.3, 7.7. IR (film) 3324, 2927, 1649, 1519, 1072, 955, 783, 680 cm^{-1}. MS (ESI) m/z: 502.3 $[M+H]^+$, 479.3, 465.3, 452.9, 413.3; HRMS (ESI) m/z $[M+H]^+$ calcd for $C_{22}H_{44}N_5O_6Si$: 502.3055, found: 502.3055.

Synthesis of benzyl (2S,4R)-4-((1-(2-(bis(3-(triethoxysilyl)propyl)amino)ethyl)-1H-1,2,3-triazol-4-yl)methoxy)-2-(((S)-1-hydroxy-3-methylbutan-2-yl)carbamoyl)pyrrolidine-1-carboxylate, ***8***. To a dry Schlenk flask equipped with a stir bar and under nitrogen atmosphere, CuI (7.6 mg, 0.04 mmol), TBTA (21.2 mg, 0.04 mmol) and anhydrous THF (10 mL) were added. The resulting mixture was stirred for 30 min. This solution was transferred to another dry Schlenk flask, equipped with a reflux condenser and under nitrogen atmosphere, containing a solution of **4** (777 mg, 2.0 mmol) in anhydrous THF (10 mL). Then, a mixture of **7** (990 mg, 2.0 mmol) and anhydrous Et_3N (1.0 mL, 0.73 g/mL, 7.2 mmol) was added by using a syringe. The resulting mixture was stirred at 80 ºC (N_2 atmosphere) until **4** was fully consumed (16 h, TLC monitoring). Then, the solvent was evaporated under reduced pressure and the residue was washed with anhydrous pentane to provide **8** as colorless oil (1.77 g, 100 % yield). $[\alpha]_D^{20}$ = -34 º (*c* 0.01, CH_2Cl_2). ^1H NMR (360 MHz, $CDCl_3$) (mixture of rotamers) δ 7.62 (s, 1H), 7.34 (br s, 5H), 6.71 (br, 0.61H), 6.07 (br s, 0.18H), 5.17-5.08 (m, 2H), 4.60 (s, 2H), 4.45-4.29 (m, 4H), 3.83 (q, *J* = 7.2 Hz , 12H), 3.74-3.59 (m, 4H), 2.88 (t, *J* = 7.2 Hz, 2H), 2.48-2.44 (m, 4H), 2.20 (br s, 1H), 1.87-1.83 (m, 1H), 1.50-1.46 (m, 4H), 1.21 (t, *J* = 7.2 Hz, 18H), 0.87 (t, *J* = 7.2 Hz, 6H), 0.56-0.51 (m, 4H), OH was not detected; ^{13}C NMR (91 MHz, $CDCl_3$) (mixture of rotamers) δ 171.9, 156.4, 144.1, 136.2, 128.5, 128.2, 127.9, 123.3, 77.3, 67.5, 63.8, 62.6, 59.6, 58.4, 57.7, 57.0, 54.2, 51.8, 48.9, 34.2, 28.9, 20.3, 19.5, 18.3, 7.8. IR (film) 3308, 2927, 1702, 1542, 1415, 1293, 1220, 1073, 953, 768, 697 cm^{-1}. MS (ESI) m/z: 883.5 $[M+H]^+$, 861.0, 847.0, 553.3, 453.3, 413.3; HRMS (ESI) m/z $[M+H]^+$ calcd for $C_{41}H_{75}N_6O_{11}Si_2$: 883.5027, found: 883.5019.

Synthesis of (2S,4R)-4-((1-(2-(bis(3-(triethoxysilyl)propyl)amino)ethyl)-1H-1,2,3-triazol-4-yl)methoxy)-N-((S)-1-hydroxy-3-methylbutan-2-yl)pyrrolidine-2-carboxamide, ***P2***. A mixture of **8** (1.79 g, 2.0 mmol) and 426 mg of 10% Pd/C (0.4 mmol Pd, 20 mol%) in absolute ethanol (20 mL) was hydrogenated at 60 ºC under 3 atm of H_2 for 48 h. The mixture was filtered through Celite® 545, and the solvent from filtrate was evaporated at reduced pressure to afford **P2** as a colorless oil (1.38 mg, 92% yield). $[\alpha]_D^{20}$ = -12 º (*c* 0.01, CH_2Cl_2). ^{1}H NMR (600 MHz, $CDCl_3$) δ 7.96 (d, *J* = 7.8 Hz, 1H), 7.66 (s, 1H), 4.56 (d, *J* = 11.8 Hz, 1H), 4.52 (d, *J* = 11.8 Hz, 1H), 4.37 (t, *J* = 6.3 Hz, 2H), 4.14 (br, 1H), 4.01 (t, *J* = 8.4 Hz, 1H), 3.77 (q, *J* = 7.0 Hz, 12H), 3.67-3.58 (m, 3H), 3.21 (d, *J* = 12.8 Hz, 1H), 2.88 (t, *J* = 6.3 Hz, 2H), 2.80 (dd, *J* = 12.8 and 2.5 Hz, 1H), 2.47-2.41 (m, 5H), 1.92 (m, 1H), 1.87 (m, 1H), 1.47 (m, 4H), 1.18 (t, *J* = 7.0 Hz, 18H), 0.90 (d, *J* = 6.7 Hz, 3H), 0.86 (d, *J* = 6.7 Hz, 3H), 0.50 (m, 4H), OH was not detected; ^{13}C NMR (91 MHz, $CDCl_3$) δ 176.0, 144.5, 123.3, 80.7, 64.9, 62.1, 59.9, 58.4, 57.4, 57.1, 54.2, 52.4, 48.9, 36.5, 29.0, 20.3, 19.7, 18.5, 18.3, 7.8. IR (film) 3324, 2927, 1655, 1523, 1389, 1100, 1073, 953, 770 cm^{-1}. MS (ESI) m/z: 749.5 $[M + H]^+$, 618.4, 551.3, 452.3, 413.7, 375.2, 259.2; HRMS (ESI) m/z $[M + H]^+$ calcd for $C_{33}H_{69}N_6O_9Si_2$: 749.4659, found: 749.4656.

Preparation of mesoporous silica nanoparticles ***MCM-41***.[54] In an open 250 mL round bottom flask without reflux condenser was placed a solution of cetyltrimethylammonium bromide (CTAB, 315 mg, 0.86 mmol) in Mili-Q water (150 mL). Then a solution of 2 M NaOH (1.1 mL, 2.2 mmol) was added, causing the pH to increase to above 12 and inducing the complete dissolution of CTAB. The mixture was stirred at 1000 rpm at 80 °C while stirring to create a homogeneous solution. Tetraethyl orthosilicate (TEOS, 1.4 mL, 6.28 mmol) was added to the solution dropwise. The condensation process was conducted for two hours at 80 °C under stirring. The suspension was cooled to room temperature while stirring and the NPs were collected by centrifugation (13500 rpm at 25°C for 45 mins). In order to remove the surfactant, 20 mL of an alcoholic solution of ammonium nitrate [NH_4NO_3, 6 g/L in 96% EtOH] was added

to each tube. The tubes were sonicated for 30 min at 50 °C, then cooled and centrifuged (30 min at 13500 rpm at 25 °C), the supernatant was discarded. This NH_4NO_3 washing was performed 3 times. Each solid in the tubes was washed successively with 96% ethanol, Mili-Q water, 96% ethanol using the same protocol (30 min at 50 °C sonication, centrifugation). The final product was dried for few hours under vacuum at room temperature. The MCM-41 silica nanoparticles were obtained as a white solid (296 mg). BET: S_{BET} = 1097 m^2/g, V_{pore} = 0.79 cm^3g^{-1}, $\emptyset_{pore}$ = 2.7 nm. IR (ATR) ν (cm^{-1}): 3432, 1044, 959, 879, 796.

Preparation of mesoporous silica nanoparticles ***M0.***[82] MSNs were synthesized in an aqueous buffer solution of pH 7 from a mixture with the following molar ratios: Brij-56:CTAB:TEOS:H_2O = 7:20:160:120,000. Initially, CTAB (911 mg, 2.50 mmol) and Brij-56 (598 mg, 0.875 mmol) were dissolved in the buffer solution, prepared from KH_2PO_4 (858 mg, 6.3 mmol) and NaOH (145 mg, 3.625 mmol) in H_2O (270 mL, 15000 mmol), under vigorous stirring and heating at 95 ºC. When the solution became homogeneous, TEOS (4.17 g, 20 mmol) was added slowly. The reaction was maintained for 8 hours under stirring at 95ºC. The suspension was cooled to room temperature while stirring and the NPs were collected by centrifugation (13500 rpm at 25 °C for 45 mins). In order to remove the surfactant, 20 mL of an alcoholic solution of ammonium nitrate [NH_4NO_3, 6 g/L in 96% EtOH] was added to each tube, sonicated for 30 min at 50 °C, then cooled and centrifuged (30 min at 13500 rpm at 25 °C), the supernatant was discarded. This NH_4NO_3 washing was performed 3 times. Each solid in the tubes was washed successively with 96% ethanol, Mili-Q water, 96% ethanol using the same protocol (30 min at 50 °C sonication, centrifugation). The final product was dried for few hours under vacuum at room temperature. The **M0 NPs** were obtained as a white solid (940 mg). BET: S_{BET} = 332 m^2/g, V_{pore} = 0.29 cm^3g^{-1}, $\emptyset_{pore}$ = 3.1 nm. IR (ATR) ν (cm^{-1}): 2926, 1044, 966, 797, 621.

*Preparation of functionalized mesoporous silica nanoparticles **M1*.** In a 250 mL round bottom flask equipped with a Dean-Stark apparatus, compound **P1** (401.3 mg, 0.8 mmol) and mesostructured silica nanoparticles MCM-41 (481 mg, 8.0 mmol) were refluxed in dry toluene (80 mL) for 24 h. After this time the suspension was centrifuged (12000 rpm at 25 °C for 45 min). The solid was washed successively with ethanol (3 × 20 mL) and acetone (2 × 20 mL) (30 min at 50 °C sonication, 30 min for centrifugation), then dried under vacuum and finally crushed to give the grafted material **M1** as a white solid (450 mg). Elemental analysis: 5.43% N, 17.74% C, 2.95% H (0.78 mmol prolinamide/g material). BET: S_{BET} = 682 m^2/g, V_{pore} = 0.29 cm^3g^{-1}, $\emptyset_{pore}$ = 2.6 nm**.** IR (ATR) ν (cm^{-1}): 3323, 1648, 1534, 1056, 961, 796. ^{13}C CP MAS NMR (100.6 MHz) *δ*: 177.1, 144.8, 125.0, 80.3, 60.2, 57.8, 52.6, 36.9, 29.8, 24.8, 17.7, 17.0, 7.9; ^{29}Si CP MAS NMR (79.5 MHz) *δ*: -60 (T^2), -68 (T^3), -93 (Q^2), -103 (Q^3), -113 (Q^4).

*Preparation of functionalized mesoporous silica nanoparticles **M2***. In a 250 mL round bottom flask equipped with a Dean-Stark apparatus, compound **P2** (599 mg, 0.80 mmol) and mesostructured silica nanoparticles MCM-41 (481 mg, 8.0 mmol) were refluxed in dry toluene (80 mL) for 24 h. After this time the suspension was centrifuged (12000 rpm at 25 °C for 45 min). The solid was washed successively with ethanol (3 × 20 mL) and acetone (2 × 20 mL), (30 min at 50 °C sonication, 30 min for centrifugation), then dried under vacuum and finally crushed to give the grafted material **M2** as a white solid (620 mg). Elemental analysis: 5.84% N, 21.76% C, 3.63% H (0.69 mmol prolinamide/g material). BET: S_{BET} = 477 m^2/g, V_{pore} = 0.21 cm^3g^{-1}, $\emptyset_{pore}$ = 2.5 nm. IR (ATR) ν (cm^{-1}): 3320, 2923, 1655, 1531, 1464, 1221, 1050, 795. ^{13}C CP MAS NMR (100.6 MHz) *δ*: 176.2, 145.3, 124.1, 79.0, 58.2, 29.9, 17.3, 9.6.

*Preparation of functionalized mesoporous silica nanoparticles **M3***. In a 250 mL round bottom flask equipped with a Dean-Stark apparatus, compound **P1** (634 mg, 1.26 mmol) and mesostructured silica nanoparticles **M0** (759.2 mg, 12.6 mmol) were refluxed in dry toluene (120 mL) for 24 h. After this time the suspension was centrifuged (12000 rpm at 25 °C for 45

min). The solid was washed successively with ethanol (3 × 20 mL) and acetone (2 × 20 mL) (30 min at 50 °C sonication, 30 min for centrifugation), then dried under vacuum and finally crushed to give the grafted material **M3** as a white solid (760 mg). Elemental analysis: 3.33% N, 15.63% C, 2.76% H (0.48 mmol prolinamide/g material). BET: S_{BET} = 183 m^2/g, V_{pore} = 0.14 cm^3g^{-1}, $\emptyset_{pore}$ = 3.0 nm. IR (ATR) ν (cm^{-1}): 2925, 1654, 1529, 1466, 1050, 795. ^{13}C CP MAS NMR (100.6 MHz) δ: 176.8, 145.3, 126.0, 80.9, 67.9, 58.2, 53.9, 30.1, 23.1, 17.6, 8.7; ^{29}Si CP MAS NMR (79.5 MHz) δ: -60 (T^2), -69 (T^3), -95 (Q^2), -103 (Q^3), -113 (Q^4).

*Preparation of functionalized mesoporous silica nanoparticles **M4***. In a 250 mL round bottom flask equipped with a Dean-Stark apparatus, compound **P2** (944 mg, 1.26 mmol) and mesostructured silica nanoparticles **M0** (759 mg, 12.6 mmol) were refluxed in dry toluene (120 mL) for 24 h. After this time the suspension was centrifuged (12000 rpm at 25 °C for 45 min). The solid was washed successively with ethanol (3 × 20 mL) and acetone (2 × 20 mL) (30 min at 50 °C sonication, 30 min for centrifugation), then dried under vacuum and finally crushed to give the grafted material **M4** as a white solid (718 mg). Elemental analysis: 3.07% N, 15.60% C, 2.80% H (0.37 mmol prolinamide/g material). BET: S_{BET} = 177 m^2/g, V_{pore} = 0.13 cm^3g^{-1}, $\emptyset_{pore}$ = 3.0 nm. IR (ATR) ν (cm^{-1}): 2926, 1655, 1529, 1467, 1049, 794. ^{13}C CP MAS NMR (100.6 MHz) δ: 176.7, 144.8, 127.8, 80.4, 67.1, 57.9, 53.9, 30.1, 23.0, 17.4, 8.2.

*Preparation of functionalized mesoporous silica nanoparticles **M5**.* MSNs were synthesized in an aqueous buffer solution of pH 7 from a mixture with the following molar ratios: Brij-56:CTAB:TEOS:**P1**:H_2O = 7:20:160:16:120,000. Initially, CTAB (455mg, 1.25 mmol) and Brij-56 (299 mg, 0.438 mmol) were dissolved in the buffer solution, prepared from KH_2PO_4 (429 mg, 3.15 mmol) and NaOH (72.5 mg, 1.81 mmol) in H_2O (135 mL, 7500 mmol), under vigorous stirring (1000 rpm) and heating at 95 ºC. When the solution became homogeneous, a mixture of TEOS (2.08 g, 10 mmol) and **P1** (502mg, 1.0 mmol) was added slowly. The reaction was maintained for 8 hours under stirring at 95ºC. The suspension was cooled to room

temperature while stirring and the NPs were collected by centrifugation (13500 rpm at 25 °C for 45 mins). In order to remove the surfactant, 20 mL of an alcoholic solution of ammonium nitrate [NH_4NO_3, 6 g/L in 96% EtOH] was added to each tube, sonicated for 30 min at 50 °C, then cooled and centrifuged (30 min at 13500 rpm at 25 °C), the supernatant was discarded. This NH_4NO_3 washing was performed 3 times. Each solid in the tubes was washed successively with 96% ethanol, Mili-Q water, 96% ethanol using the same protocol (30 min at 50 °C sonication, centrifugation). The white solid material **M5** was dried for few hours under vacuum at room temperature (541 mg). Elemental analysis: 5.71% N, 17.22% C, 3.04% H (0.82 mmol prolinamide/g material). BET: S_{BET} = 135 m^2/g, V_{pore} = 0.09 cm^3g^{-1}, $\emptyset_{pore}$ = 2.5 nm. IR (ATR) ν (cm^{-1}): 3308, 2964, 1649, 1532, 1466, 1046, 794. ^{13}C CP MAS NMR (100.6 MHz) δ: 176.8, 144.7, 125.7, 81.7, 59.9, 58.0, 52.2, 46.1, 38.1, 29.6, 26.2, 24.2, 17.9, 8.5; ^{29}Si CP MAS NMR (79.5 MHz) δ: -59 (T^2), -69 (T^3), -94 (Q^2), -103 (Q^3), -113 (Q^4).

*Preparation of functionalized mesoporous silica nanoparticles **M6**.* MSNs were synthesized in an aqueous buffer solution of pH 7 from a mixture with the following molar ratios: Brij-56:CTAB:TEOS:**P2**:H_2O = 7:20:160:**16**:120,000. Initially, CTAB (455 mg, 1.25 mmol) and Brij-56 (299 mg, 0.438 mmol) were dissolved in the buffer solution, prepared from KH_2PO_4 (429 mg, 3.15 mmol) and NaOH (72.5 mg, 1.81 mmol) in H_2O (135 mL, 7500 mmol), under vigorous stirring (1000 rpm) and heating at 95 ºC. When the solution became homogeneous, a mixture of TEOS (2.08 g, 10 mmol) and **P2** (749 mg, 1.0 mmol) was added slowly. The reaction was maintained for 8 hours under stirring at 95ºC. The suspension was cooled to room temperature while stirring and the NPs were collected by centrifugation (13500 rpm at 25 °C for 45 mins). In order to remove the surfactant, the samples were then treated three times with a solution of NH_4NO_3 (6 g/L in 96% EtOH), and washed three times with 96% ethanol, Mili-Q water, 96% ethanol, respectively. Treatment with NH_4NO_3 and the following steps were identical as those described for **M5**. The material **M6** was obtained as a white solid (1.26 g).

Elemental analysis: 6.70% N, 19.89% C, 3.64% H (0.80 mmol prolinamide/g material). S_{BET} = 16 m^2/g, V_{pore} = 0.02 cm^3g^{-1}, $\emptyset_{pore}$ = - nm. IR (ATR) ν (cm^{-1}): 3386, 1640, 1542, 1467, 1048, 789, 712. ^{13}C CP MAS NMR (100.6 MHz) δ: 174.1, 144.6, 126.4, 78.9, 58.2, 36.1, 29.4, 19.9, 19.0, 9.9; ^{29}Si CP MAS NMR (79.5 MHz) δ: -59 (T^2), -68 (T^3), -93 (Q^2), -103 (Q^3), -113 (Q^4).

*Typical procedure for catalytic test in asymmetric aldol reaction with functionalized mesoporous silica nanoparticles***.** In a vial, cyclic ketone (2.5 mmol), mili-Q water (250 μL) and the supported catalyst (10 mol%, 0.05 mmol) were stirred together for 20 min at 0 ºC. After this time, the aldehyde (0.5 mmol) was added and the mixture was stirred until TLC showed complete consumption of the aldehyde. Then the crude mixture was diluted with EtOAc (10 mL) and centrifuged (4000 rpm, 15 min). The resulting solid catalytic material was washed several times with EtOAc (3 × 10 mL) and the combined supernatants were concentrated under vacuum. From this residue, the conversion, the *anti/syn* ratio of the diastereomeric mixture and enantiomeric ratio (*er*) were determined. The solid catalytic material that had been collected by centrifugation and washed with EtOAc was then dried under vacuum and directly used in the next cycle.

Spectroscopic data for aldol compounds ***anti-11***

2-(Hydroxy-(4-nitrophenyl)methyl)cyclohexan-1-one, ***11aa***[85]

^1H NMR (360 MHz, $CDCl_3$) δ 8.22 (d, *J* = 7.2 Hz, 2H), 7.52 (d, *J* = 7.2 Hz, 2H), 4.90 (dd, *J* = 7.2 and 3.6 Hz, 1H), 2.62-2.55 (m, 1H), 2.52-2.48 (m, 1H), 2.41-2.32 (m, 1H), 2.15-2.08 (m, 1H), 1.85-1.81 (m, 1H), 1.70-1.54 (m, 3H), 1.44-1.35 (m, 1H); ^{13}C NMR (91 MHz, $CDCl_3$) δ 214.8, 148.3, 147.6, 127.9, 123.6, 74.0, 57.2, 42.7, 30.7, 27.6, 24.7.

2-(Hydroxy-(2-nitrophenyl)methyl)cyclohexan-1-one, ***11ab***[86]

Purification by flash chromatography on silica gel with hexane/AcOEt (3/1) as eluent, white solid. ^1H NMR (360 MHz, $CDCl_3$) δ 7.86 (d, *J* = 7.2 Hz, 1H), 7.78 (d, *J* = 7.2 Hz, 1H), 7.64 (t, *J* = 7.2 Hz, 1H), 7.43 (t, *J* = 7.2 Hz, 1H), 5.43 (d, *J* = 7.2 Hz, 1H), 4.18 (br s, 1H), 2.79-2.71

(m, 1H), 2.50-2.43 (m, 1H), 2.38-2.29 (m, 1H), 2.12-2.04 (m, 1H), 1.87-1.83 (m, 1H), 1.78-1.53 (m, 4H); ^{13}C NMR (91 MHz, $CDCl_3$) δ 215.0, 148.1, 136.6, 133.1, 129.0, 128.4, 124.1, 69.8, 57.3, 42.8, 31.1, 27.8, 25.0.

2-(Hydroxy-(2,4-dinitrophenyl)methyl)cyclohexan-1-one, ***11ac***[87]

Purification by flash chromatography on silica gel with hexane/AcOEt (2/1) as eluent, white solid. ^{1}H NMR (360 MHz, $CDCl_3$) δ 8.75 (d, J = 2.2 Hz, 1H), 8.48 (dd, J = 7.2 and 3.6 Hz, 1H), 8.08 (d, J = 7.2 Hz, 1H), 5.52 (t, J = 5.8 Hz, 1H), 4.30 (d, J = 7.2 Hz, 1H), 2.76-2.71 (m, 1H), 2.48-2.44 (m, 1H), 2.36-2.28 (m, 1H), 2.15-2.11 (m, 1H), 1.92-1.56 (m, 5H); ^{13}C NMR (91 MHz, $CDCl_3$) δ 214.5, 148.2, 147.0, 143.9, 131.0, 127.1, 119.9, 70.2, 56.9, 42.9, 31.4, 27.7, 25.0.

2-((4-Chlorophenyl)(hydroxy)methyl)cyclohexan-1-one, ***11ad***[88]

Purification by flash chromatography on silica gel with hexane/AcOEt (4/1) as eluent, white solid. ^{1}H NMR (360 MHz, $CDCl_3$) δ 7.33-7.31 (m, 2H), 7.27-7.24 (m, 2H), 4.77 (dd, J =7.2 and 3.6 Hz, 1H), 4.00 (d, J = 3.6 Hz, 1H), 2.59-2.45 (m, 2H), 2.40-2.31 (m, 1H), 2.13-2.06 (m, 1H), 1.82-1.78 (m, 1H), 1.71-1.48 (m, 3H), 1.34-1.21 (m, 1H); ^{13}C NMR (91 MHz, $CDCl_3$) δ 215.4, 139.5, 133.6, 128.5, 128.4, 74.1, 57.4, 42.7, 30.7, 27.7, 24.7.

2-((4-Fluorophenyl)(hydroxy)methyl)cyclohexan-1-one, ***11ae***[86]

Purification by flash chromatography on silica gel with hexane/AcOEt (4/1) as eluent, white solid. ^{1}H NMR (360 MHz, $CDCl_3$) δ 7.31-7.27 (m, 2H), 7.06-7.01 (m, 2H), 4.79 (dd, J =7.2 and 3.6 Hz, 1H), 4.00 (d, J = 3.6 Hz, 1H), 2.57-2.47 (m, 2H), 2.39-2.35 (m, 1H), 2.09-2.07 (m, 1H), 1.82-1.78 (m, 1H), 1.68-1.53 (m, 3H), 1.30-1.26 (m, 1H); ^{13}C NMR (91 MHz, $CDCl_3$) δ 215.5, 128.7, 128.6, 115.4, 115.1, 74.1, 57.5, 42.7, 30.8, 27.7, 24.7.

2-((4-Bromophenyl)(hydroxy)methyl)cyclohexan-1-one, ***11af***[88]

Purification by flash chromatography on silica gel with hexane/AcOEt (5/1) as eluent, white solid. ^{1}H NMR (360 MHz, $CDCl_3$) δ 7.49 (d, J = 10.8 Hz, 2H), 7.21 (d, J = 7.2 Hz, 2H), 4.77

(dd, *J* =7.2 and 3.6 Hz, 1H), 4.00 (d, *J* = 3.6 Hz, 1H), 2.59-2.46 (m, 2H), 2.40-2.31 (m, 1H), 2.13-2.05 (m, 1H), 1.82-1.78 (m, 1H), 1.72-1.49 (m, 3H), 1.36-1.23 (m, 1H); ^{13}C NMR (91 MHz, $CDCl_3$) δ 215.3, 140.0, 131.5, 128.7, 121.7, 74.2, 57.3, 42.7, 30.7, 27.7, 24.7

2-((2-Chlorophenyl)(hydroxy)methyl)cyclohexan-1-one, ***11ag***[85]

^{1}H NMR (360 MHz, $CDCl_3$) δ 7.56-7.54 (m, 1H), 7.35-7.29 (m, 1H), 7.24-7.19 (m, 1H), 7.43 (t, *J* = 7.2 Hz, 1H), 4.04 (d, *J* = 7.2 Hz, 1H), 2.72-2.65 (m, 1H), 2.49-2.45 (m, 1H), 2.38-2.32 (m, 1H), 2.11-2.07 (m, 1H), 1.90-1.82 (m, 1H), 1.75-1.52 (m, 4H); ^{13}C NMR (91 MHz, $CDCl_3$) δ 215.3, 139.0, 133.0, 129.2, 128.7, 128.2, 127.2, 70.4, 57.6, 42.7, 30.4, 27.8, 24.9.

2-((2,4-Dichlorophenyl)(hydroxy)methyl)cyclohexan-1-one, ***11ah***[86]

^{1}H NMR (360 MHz, $CDCl_3$) δ 7.51 (d, *J* = 7.2 Hz, 1H), 7.36 (d, *J* = 3.6 Hz, 1H), 7.31-7.27 (m, 1H), 5.30 (d, *J* = 7.2 Hz, 1H), 4.06 (br s, 1H), 2.66-2.59 (m, 1H), 2.49-2.45 (m, 1H), 2.38-2.29 (m, 1H), 2.12-2.08 (m, 1H), 1.90-1.83 (m, 1H), 1.73-1.56 (m, 4H); ^{13}C NMR (91 MHz, $CDCl_3$) δ 215.1, 137.8, 133.8, 133.5, 129.2, 128.9, 127.6, 70.1, 57.5, 42.7, 30.4, 27.8, 24.9.

2-(Hydroxy-(4-(trifluoromethyl)phenyl)methyl)cyclohexan-1-one, ***11ai***[89]

^{1}H NMR (360 MHz, $CDCl_3$) δ 7.62- (d, *J* = 7.2 Hz, 2H), 7.45 (d, *J* = 7.2 Hz, 2H), 4.86 (d, *J* =7.2 Hz, 1H), 4.01 (br s, 1H), 2.63-2.56 (m, 1H), 2.51-2.46 (m, 1H), 2.41-2.31 (m, 1H), 1.89-1.78 (m, 1H), 1.75-1.48 (m, 3H), 1.39-1.25 (m, 1H); ^{13}C NMR (91 MHz, $CDCl_3$) δ 215.1, 145.0, 130.2 (q, *J* = 32.8 Hz), 127.4, 125.4 (q, *J* = 3.6 Hz), 122.6 (q, *J* = 318 Hz), 74.3, 57.3, 42.7, 30.8, 27.7, 24.7.

3-(hydroxy-(4-nitrophenyl)methyl)tetrahydro-4H-pyran-4-one, ***11ba***[90]

^{1}H NMR (360 MHz, $CDCl_3$) δ 8.24 (d, *J* = 7.2 Hz, 2H), 7.50 (d, *J* = 7.2 Hz, 2H), 5.00 (d, *J* = 7.2 Hz, 1H), 4.23-4.18 (m, 1H), 3.83 (br s, 1H), 3.79-3.70 (m, 2H), 3.48-3.42 (m, 1H), 2.92-2.86 (m, 1H), 2.73-2.64 (m, 1H), 2.56-2.48 (m, 1H); ^{13}C NMR (91 MHz, $CDCl_3$) δ 209.3, 147.8, 147.4, 127.5,126.4, 123.9, 123.7, 71.3, 69.8, 68.4, 57.6, 42.9.

ASSOCIATED CONTENT

Supporting Information

NMR characterization of silylated precursors **P1** and **P2**

Characterization of functionalized mesoporous silica nanoparticles **M1**-**M6**

Recycling experiments with **M1** and **M5**

Kinetics studies of the direct asymmetric aldol reaction of aldehyde **9a** with cyclohexanone **10a** catalyzed by **M1**

NMR spectra of compounds

Table of ^{1}H NMR of C*H*OH proton, HPLC conditions and retention times for compounds **11**

HPLC chromatograms of compounds ***anti*-11**

AUTHOR INFORMATION

Corresponding author

E-mail: roser.pleixats@uab.cat

ORCID: 0000-0003-2544-732X

Author Contributions

The manuscript was written through contributions of all authors. All authors have given approval to the final version of the manuscript.

Funding Sources

CNRS (France)

Ministerio de Economía, Industria y Competitividad (MINECO) of Spain (Projects CTQ2014-53662-P and CTQ2016-81797-REDC)

Ministerio de Ciencia, Innovación y Universidades (MCIU) of Spain (Project RTI2018-097853-B-I00)

DURSI-Generalitat de Catalunya (Project SGR2017-0465)

China Scholarship Council (CSC) (predoctoral scholarship to Hao Li, CSC No. 201606890025)

Notes

The authors declare no competing financial interest

ACKNOWLEDGEMENTS

We are thankful for financial support from CNRS (France), Ministerio de Economía, Industria y Competitividad (MINECO) of Spain (Projects CTQ2014-53662-P and CTQ2016-81797-REDC), Ministerio de Ciencia, Innovación y Universidades (MCIU) of Spain (Project RTI2018-097853-B-I00), DURSI-Generalitat de Catalunya (Project SGR2017-0465), and China Scholarship Council (CSC) for a predoctoral scholarship to Hao Li.

REFERENCES

(1) Dalko, P. I., Ed. Enantioselective Organocatalysis: Reactions and Experimental Procedures; Wiley-VCH: Weinheim, 2007.

(2) Special issue: Houk, K. N.; List, B., Guest Eds. Asymmetric Organocatalysis. *Acc. Chem. Res.* **2004**, *37* (8), 487-631.

(3) Special issue: Kocovsky, P.; Malkov, A. V. Guest Eds. Organocatalysis in Organic Synthesis. *Tetrahedron* **2006**, *62* (2-3), 243-502.

(4) Special issue: List, B. Guest Ed. Organocatalysis. *Chem. Rev.* **2007**, *107* (12), 5413-5883.

(5) Dalko, P. I.; Moisan, L. In the Golden Age of Organocatalysis. *Angew. Chem. Int. Ed.* **2004,** *43* (39), 5138-5175.

(6) Pellissier, H. Asymmetric Organocatalysis. *Tetrahedron* **2007**, *63* (38), 9267-9331.

(7) Mukherjee, S.; Yang, J. W.; Hoffmann, S.; List, B. Asymmetric Enamine Catalysis. *Chem. Rev*. **2007**, *107* (12), 5471-5569.

(8) Sulzer-Mossé, S.; Alexakis, A. Chiral Amines as Organocatalysts for Asymmetric Conjugate Addition to Nitroolefins and Vinyl Sulfones via Enamine Activation. *Chem. Commun*. **2007**, (30), 3123-3135.

(9) Erkkilä, A.; Majander, I.; Pihko, P. M. Iminium Catalysis. *Chem. Rev*. **2007**, *107* (12), 5416-5470.

(10) Ting, A.; Schaus, S. E. Organocatalytic Asymmetric Mannich Reactions: New Methodology, Catalyst Design, and Synthetic Applications. *Eur. J. Org. Chem*. **2007**, (35), 5797-5815.

(11) Guillena, G.; Ramón, D. J.; Yus, M. Organocatalytic Enantioselective Multicomponent Reactions (OEMCRs). *Tetrahedron:Asymmetry* **2007**, 18 (6), 693-700.

(12) Melchiorre, P.; Marigo, M.; Carlone, A.; Bartoli, G. Asymmetric Aminocatalysis-Gold Rush in Organic Chemistry. *Angew. Chem. Int. Ed*. **2008**, *47* (33), 6138-6171.

(13) MacMillan, D. W. C. The Advent and Development of Organocatalysis. *Nature* **2008**, *455* (7211), 304-308.

(14) Dondoni, A.; Massi, A. Asymmetric Organocatalysis: from Infancy to Adolescence. *Angew. Chem. Int. Ed*. **2008**, *47* (25), 4638-4660.

(15) Bertelsen, S.; Jørgensen, K. A. Organocatalysis-After the Gold Rush. *Chem. Soc. Rev.* **2009**, *38* (8), 2178-2189.

(16) Palomo, C.; Oiarbide, M.; López, R. Asymmetric Organocatalysis by Chiral Brønsted Bases: Implications and Applications. *Chem. Soc. Rev*. **2009**, *38* (2), 632-653.

(17) Liu, X.; Lin, L.; Feng, X. Amide-Based Bifunctional Organocatalysts in Asymmetric Reactions. *Chem. Commun*. **2009**, (41), 6145-6158.

(18) Giacalone, F.; Gruttadauria, M.; Agrigento, P.; Noto, R. Low-Loading Asymmetric Organocatalysis. *Chem. Soc. Rev*. **2012**, *41* (6), 2406-2447.

(19) Meninno, S.; Lattanzi, A. Asymmetric Organocatalysis Mediated by α,α-L-Diaryl Prolinols: Recent Advances. *Chem. Commun.* **2013**, *49* (37), 3821-3832.

(20) Albrecht, L.; Jiang, H.; Jørgensen, K. A. Hydrogen-Bonding in Aminocatalysis: From Proline and Beyond. *Chem. Eur. J*. **2014**, *20* (2), 358-368.

(21) (q) Liu, J.; Wang, L. Recent Advances in Asymmetric Reactions Catalyzed by Proline and Its Derivatives. *Synthesis* **2017**, *49* (5), 960-972.

(22) Klier, L.; Tur, F.; Poulsen, P. H.; Jørgensen, K. A. Asymmetric Cycloaddition Reactions Catalysed by Diarylprolinol Silyl Ethers. *Chem. Soc. Rev*. **2017**, *46* (4), 1080-1102.

(23) Heravi, M. M. ; Zadsirjan, V.; Dehghani, M.; Hosseintash, N. Current Applications of Organocatalysts in Asymmetric Aldol Reactions : An Update. *Tetrahedron: Asymmetry* **2017**, *28* (5), 587-707.

(24) Alonso, D. A.; Baeza, A.; Chinchilla, R.; Gómez, C.; Guillena, G.; Pastor, I. M.; Ramón, D. J. Recent Advances in Asymmetric Organocatalysed Conjugate Additions to Nitroalkenes. *Molecules* **2017**, *22* (6), 895 (1-51).

(25) Yin, Y.; Jiang, Z. Organocatalytic Asymmetric Vinilogous Michael Reactions. *ChemCatChem* **2017**, *9* (23), 4306-4318.

(26) Chanda, T.; Zhao, J. C.-G. Recent Progress in Organocatalytic Asymmetric Domino Transformations. *Adv. Synth. Catal.* **2018**, *360* (1), 2-79.

(27) Marcia de Figueiredo, R.; Christmann, M. Organocatalytic Synthesis of Drugs and Bioactive Natural Products. *Eur. J. Org. Chem.* **2007**, (16), 2575-2600.

(28) Alemán, J.; Cabrera, S. Applications of Asymmetric Organocatalysis in Medicinal Chemistry. *Chem. Soc. Rev.* **2013**, *42* (2), 774-793.

(29) Guillena, G.; Nájera, C.; Ramón, D. J. Enantioselective Direct Aldol Reaction: Te Blossoming of Modern Organocatalysis. *Tetrahedron: Asymmetry* **2007**, *18* (19), 2249-2293.

(30) Trost, B. M.; Brindle, C. S. The Direct Catalytic Asymmetric Aldol Reaction. *Chem. Soc. Rev*. **2010**, *39* (5), 1600-1632.

(31) Mase, N.; Barbas III, C. F. In Water, on Water, and by Water: Mimicking Nature's Aldolases with Organocatalysis and Water. *Org. Biomol. Chem*. **2010**, *8* (18), 4043-4050.

(32) Jimeno, C. Water in Asymmetric Organocatalytic Systems. A Global Perspective. *Org. Biomol. Chem*. **2016**, *14* (26), 6147-6164.

(33) Wang, B.; Chen, G.-H.; Liu, L.-Y.; Chang, W.-X.; Li, J. A Novel Proline-Valinol Thioamide Small Organic Molecule for a Highly Enantioselective Direct Aldol Reaction. *Adv. Synth. Catal*. **2009**, *351* (14-15), 2441-2448.

(34) Benaglia, M.; Puglisi, A.; Cozzi, F. Polymer-Supported Organic Catalysts. *Chem. Rev*. **2003**, *103* (9), 3401-3430.

(35) Cozzi, F. Immobilization of Organic Catalysts: When, Why, and How. *Adv. Synth. Catal*. **2006**, *348* (12-13), 1367-1390.

(36) Benaglia, M. Recoverable and Recyclable Chiral Organic Catalysts. *New J. Chem.* **2006**, *30* (11), 1525-1533.

(37) Gruttadauria, M.; Giacolone, F.; Noto, R. Supported Proline and Proline-Derivatives as Recyclable Organocatalysts. *Chem. Soc. Rev*. **2008**, *37* (8), 1666-1688.

(38) Kristensen, T. E.; Hansen, T. Polymer-Supported Chiral Organocatalysts: Synthesis, Strategies for the Road Towards Affordable Polymeric Immobilization. *Eur. J. Org. Chem*. **2010**, (17), 3179-3204.

(39) Puglisi, A.; Benaglia, M.; Chiroli, V. Stereoselective Organic Reactions Promoted by Immobilized Chiral Catalysts in Continuous Flow Systems. *Green Chem*. **2013**, *15* (7), 1790-1813.

(40) Rodríguez-Escrich, C.; Pericàs, M. A. Organocatalysis on Tap: Enantioselective Continuous Flow Processes Mediated by Solid-Supported Chiral Organocatalysts. *Eur. J. Org. Chem*. **2015**, (6), 1173-1188.

(41) Atodiresei, I.; Vila, C.; Rueping, M. Asymmetric Organocatalysis in Continuous Flow: Opportunities for Impacting Industrial Catalysis. *ACS Catal*. **2015**, *5* (3), 1972-1985.

(42) Ferré, M.; Pleixats, R.; Wong Chi Man, M.; Cattoën, X. Recyclable Organocatalysts Based on Hybrid Silicas. *Green Chem*. **2016**, *18* (4), 881-922.

(43) Huybrechts, W.; Lauwaert, J.; De Vylder, A.; Mertens, M.; Mali, G.; Thybaut, J. W.; Van Der Voort, P.; Cool, P. Synthesis of L-Serine Modified Benzene Bridged Periodic Mesoporous Organosilica and its Catalytic Performance Towards Aldol Condensations. *Microporous Mesoporous Mater*. **2017**, *251*, 1-8.

(44) An, Z.; Guo, Y.; Zhao, L.; Li, Zhi; He, J. L-Proline-Grafted Mesoporous Silica with Alternating Hydrophobic and Hydrophilic Blocks to Promote Direct Asymmetric Aldol and Knoewenagel-Michael Cascade Reactions. *ACS Catal*. **2014**, *4* (8), 2566-2576.

(45) Zamboulis, A.; Moitra, N.; Moreau, J. J. E.; Cattoën, X.; Wong Chi Man, M. Hybrid Materials: Versatile Matrices for Supporting Homogeneous Catalysts. *J. Mater. Chem*. **2010**, *20* (42), 9322-9338.

(46) Corma, A.; García, H. Silica-Bound Homogeneous Catalysts as Recoverable and Reusable Catalysts in Organic Synthesis. *Adv. Synth. Catal*. **2006**, *348* (12-13), 1391-1412.

(47) Brinker, C. J.; Scherer, G. W. Sol-Gel Science: the Physics and Chemistry of Sol-Gel Processing, 1st edition; Academic Press: San Diego, 1990.

(48) Slowing, I. I.; Vivero-Escoto, J. L.; Trewyn, B. G.; Lin, V. S.-Y. Mesoporous Silica Nanoparticles: Structural Design and Applications. *J. Mater. Chem.* **2010**, *20* (37), 7924-7937.

(49) Ambrogio, M. V.; Thomas, C. R.; Zhao, Y.; Zink, J. I.; Stoddart, J. F. Mechanized Silica Nanoparticles: A New Frontier in Theranostic Nanomedicine. *Acc. Chem. Res.* **2011**, *44* (10), 903-913.

(50) Chen, N.; Cheng, S.; Souris, J. S.; Chen, C.; Mou, C.; Lo, L. Theranostic Applications of Mesoporous Silica Nanoparticles and their Organic/Inorganic Hybrids. *J. Mater. Chem. B* **2013**, *1* (25), 3128-3135.

(51) Croissant, J. G.; Cattoën, X.; Wong Chi Man, M.; Durand, J.-O.; Khashab, N. M. Syntheses and Applications of Periodic Mesoporous Organosilica Nanoparticles. *Nanoscale* **2015**, *7* (48), 20318-20334.

(52) Manzano, M.; Vallet-Regí, M. Ultrasound Responsive Mesoporous Silica Nanoparticles for Biomedical Applications. *Chem. Commun*. **2019**, *55* (19), 2731-2740.

(53) Wu, S.-H.; Mou, C.-Y.; Lin, H.-P. Synthesis of Mesoporous Silica Nanoparticles. *Chem. Soc. Rev*. **2013**, *42* (9), 3862-3875.

(54) Théron, C.; Gallud, A.; Carcel, C.; Gary-Bobo, M.; Maynadier, M.; Garcia, M.; Lu, J.; Tamanoi, F.; Zink, J. I.; Wong Chi Man, M. Hybrid Mesoporous Silica Nanoparticles with the pH-Operated and Complementary H-Bonding Caps as an Autonomous Drug-Delivery System. *Chem. Eur. J.* **2014**, *20* (30), 9372-9380.

(55) Moitra, N.; Trens, P.; Raehm, L.; Durand, J.-O.; Cattoën, X.; Wong Chi Man, M. Facile Route to Functionalized Mesoporous Silica Nanoparticles by Click Chemistry. *J. Mater. Chem.* **2011**, *21* (35), 13476-13482.

(56) Huh, S.; Chen, H.-T.; Wiench, J. W.; Pruski M.; Lin, V. S.-Y. Cooperative Catalysis by General Acid and Base Bifunctionalized Mesoporous Silica Nanospheres. *Angew. Chem. Int. Ed.* **2005**, *44* (12), 1826-1830.

(57) Shylesh, S.; Wagner, A.; Seifert, A.; Ernst, S.; Thiel, W. R. Cooperative Acid-Base Effects with Functionalized Mesoporous Silica Nanoparticles: Applications in Carbon-Carbon Bond Formation Reactions. *Chem. Eur. J.* **2009**, *15* (29), 7052-7062.

(58) Kandel, K.; Althaus, S. M.; Peeraphatdit, C.; Kobayashi, T.; Trewyn, B. G.; Pruski M.; Slowing, I. I. Substrate Inhibition in the Heterogeneous Aldol Condensation: A Mechanistic Study of Supported Organocatalysts. *J. Catal*. **2012**, *291*, 63-68.

(59) Zhu, F.; Sun, X.; Lou, F.; An, L.; Zhao, P. Facile One-Pot Synthesis of Amine-Functionalized Mesoporous Silica Nanospheres for Water-Medium Knoevenagel Reaction under Microwave Irradiation. *Cat. Lett*. **2015**, *145* (4), 1072-1079.

(60) Cruz, P.; Pérez, Y.; del Hierro, I. Heterogeneous Organocatalysts Based on a Triazine-Triazole Silane Ligand. *Eur. J. Inorg. Chem*. **2018**, (38), 4206-4214.

(61) Huang, Y.; Trewyn, B. G.; Chen, H. -T.; Lin, V. S.-Y. One-Pot Reaction Cascades Catalyzed by Base- and Acid-Functionalized Mesoporous Silica Nanoparticles. *New J. Chem.* **2008**, *32* (8), 1311-1313.

(62) Huang, Y.; Xu, S.; Lin, V. S.-Y. Bifunctionalized Mesoporous Materials with Site-Separated Brønsted Acid and Base: Catalyst for a Two-Step Reaction Sequence. *Angew. Chem. Int. Ed.* **2011**, *50* (3), 661-664.

(63) Dickschat, A. T.; Behrends, F.; Bühner, M.; Ren, J.; Weiβ, M.; Eckert, H.; Studer, A. Preparation of Bifunctional Mesoporous Silica Nanoparticles by Orthogonal Click Reactions and Their Application in Cooperative Catalysis. *Chem. Eur. J.* **2012**, *18* (52), 16689-16697.

(64) Puglisi, A.; Annunziata, R.; Benaglia, M.; Cozzi, F.; Gervasini, A.; Bertacche, V.; Sala, M. C. Hybrid Inorganic-Organic Materials Carrying Tertiary Amine and Thiourea Residues

Tethered on Mesoporous Silica Nanoparticles: Synthesis, Characterization and Co-Operative Catalysis. *Adv. Synth. Catal*. **2009**, *351* (1-2), 219-229.

(65) Chen, H.-T.; Trewyn, B.; Wiench, J. W.; Pruski, M.; Lin, V. S.-Y. Urea and Thiourea-Functionalized Mesoporous Silica Nanoparticles Catalysts with Enhanced Catalytic Activity for Diels-Alder Reaction. *Top. Catal*. **2010**, *53* (3-4), 187-191.

(66) Peng, W.-H.; Lee, Y.-Y.; Wu, C.; Wu, K. C.-W. Acid-Base Bi-functionalized, Large-Pored Mesoporous Silica Nanoparticles for Cooperative Catalysis of One-Pot Cellulose-to-HMF Conversion. *J. Mater. Chem*. **2012**, *22* (43), 23181-23185.

(67) Ray, S.; Das, P.; Bhaumik, A.; Dutta, A.; Mukhopadhyay, C. Covalently Anchored Organic Carboxylic Acid on Porous Silica Nano Particle: A Novel Organometallic catalyst (PSNP-CA) for the Chromatography-Free Highly Product Selective Synthesis of Tetrasubstituted Imidazoles. *Appl. Catal. A* **2013**, *458*, 183-195.

(68) Das, P.; Ray, S.; Bhanja, P.; Bhaumik, A.; Mukhopadhyay, C. Serendipitous Observation of Liquid-Phase Size Selectivity Inside a Mesoporous Silica Nanoreactor in the Reaction of Chromene with Formic Acid. *ChemCatChem* **2018**, *10* (10), 2260- 2270.

(69) Puglisi, A.; Benaglia, M.; Annunziata, R.; Chiroli, V.; Porta, R.; Gervasini, A. Chiral Hybrid Inorganic-Organic Materials : Synthesis, Characterization, and Application in Stereoselective Organocatalytic Cycloadditions. *J. Org. Chem*. **2013**, *78* (22), 11326-11334.

(70) Trilla, M.; Pleixats, R.; Wong Chi Man, M.; C. Bied, C. Organic-Inorganic Hybrid Silica Materials Containing Imidazolium and Dihydroimidazolium Salts as Recyclable Organocatalysts for Knoevenagel Condensations. *Green Chem.* **2009**, *11* (11), 1815-1820.

(71) Guo, W.; Monge-Marcet, A.; Cattoën, X.; Shafir, A.; Pleixats, R. Sol-Gel Immobilized Aryl Iodides for the Catalytic Oxidative α-tosyloxylation of Ketones. *React. Funct. Polym*. **2013**, *73* (1), 192-199.

(72) Zamboulis, A.; Rahier, N. J.; Gehringer, M.; Cattoën, X.; Niel, G.; Bied, C.; Moreau, J. J. E.; Wong Chi Man, M. Silica-Supported L-Proline Organocatalysts for Asymmetric Aldolisation. *Tetrahedron: Asymmetry* **2009**, *20* (24), 2880-2885.

(73) Monge-Marcet, A.; Pleixats, R.; Cattoën, X.; Wong Chi Man, M; Alonso, D. A.; Almasi, D.; Nájera, C. Prolinamide Bridged Silsesquioxane as an Efficient, Eco-Compatible and Recyclable Chiral Organocatalyst. *New J. Chem*. **2011**, *35* (12), 2766-2772.

(74) Monge-Marcet, A.; Cattoën, X.; Alonso, D. A.; Nájera, C.; Wong Chi Man, M.; Pleixats, R. Recyclable Silica-Supported Prolinamide Organocatalyst for Direct Asymmetric Aldol Reaction in Water. *Green Chem*. **2012**, *14* (6), 1601-1610.

(75) Ferré, M.; Cattoën, X.; Wong Chi Man, M.; Pleixats, R. Recyclable Silica-Supported Proline Sulphonamide Organocatalysts for Asymmetric Direct Aldol Reaction. *ChemistrySelect* **2016**, *1* (16), 6741-6748.

(76) Fache, F.; Piva, O. Synthesis and Applications of the First Polyfluorous Proline Derivative. *Tetrahedron Asym*. **2003**, *14* (1), 139-143.

(77) Mihali, V.; Foschi, F.; Penso, M.; Pozzi, G. Chemoselective Synthesis of *N*-protected Alkoxyprolines Under Specific Solvation Conditions. *Eur. J. Org. Chem*. **2014**, (24), 5351-5355.

(78) Rostovtsev, V. V.; Green, L. G.; Fokin, V. V.; Sharpless, K. B. A Stepwise Huisgen Cycloaddition Process: Copper(I)-Catalyzed Regioselective Ligation of Azides and Terminal Alkynes. *Angew. Chem. Int. Ed*. **2002**, *41* (14), 2596-2599.

(79) Meldal; M.; Tornøe, C. W. Cu-Catalyzed Azide-Alkyne Cycloaddition. *Chem. Rev*. **2008**, *108* (8), 2952-3015.

(80) Bürglová, K.; Moitra, N.; Hodacová, J.; Cattoën, X.; Wong Chi Man, M. Click Approaches to Functional Water-Sensitive Organotriethoxysilanes. *J. Org. Chem*. **2011**, *76* (18), 7326-7333.

(81) Bürglová, K; Noureddine, A.; Hodacová, J.; Toquer, G.; Cattoën, X.; Wong Chi Man, M. A General Method for Preparing Bridged Organosilanes with Pendant Functional Groups and Functional Mesoporous Organosilicas. *Chem. Eur. J.* **2014**, *20* (33), 10371-10382.

(82) He, Q.-J.; Cui, X.-Z.; Cui, F.-M.; Guo, L.-M.; Shi, J.-L. Size-Controlled Synthesis of Monodispersed Mesoporous Silica Nano-Spheres Under a Neutral Condition. *Microporous Mesoporous Mater*. **2009**, *117* (3), 609-616.

(83) Kühbeck, D.; Bachl, J.; Schön, E-M.; Gotor-Fernández, V.; Díaz Díaz, D. Gelatin protein-mediated direct aldol reaction. *Helv. Chim. Acta* **2014**, *97* (4), 574-580.

(84) Zhang, Q.; Su, H.; Luo, J.; Wei, Y.-Y. Click Magnetic Nanoparticle-Supported Palladium Catalyst: A Phosphine-Free, Highly Efficient and Magnetically Recoverable Catalyst for Suzuki-Miyaura Coupling Reactions. *Catal. Sci. Technol*. **2013**, *3* (1), 235-243.

(85) Almaşi, D.; Alonso, D. A.; Nájera, C. Prolinamides *versus* Prolinethioamides as Recyclable Catalysts in the Enantioselective Solvent-Free Inter- and Intramolecular Aldol Reactions. *Adv. Synth. Catal.* **2008**, *350* (16), 2467-2472.

(86) Li, Z.-Y.; Chen, Y.; Zheng, C.-Q.; Yin, Y.; Wang, L.; Sun, X.-Q. Highly Enantioselective Aldol Reactions Catalyzed by Reusable Upper Rim-Functionalized Calix[4]arene-Based L-Proline Organocatalyst in Aqueous Conditions. *Tetrahedron* **2017**, *73* (1), 78-85.

(87) Zhang, X.; Zhao, W.-S.; Qu, C.-K.; Yang, L.-L.; Cui, Y.-C. Efficient Asymmetric Aldol Reaction Catalyzed by Polyvinylidene Chloride-Supported Ionic Liquid/ L-Proline Catalyst System. *Tetrahedron: Asymmetry* **2012**, *23* (6-7), 468-473.

(88) Hernández, J. G.; Juaristi, E. Asymmetric Aldol Reaction Organocatalyzed by (*S*)-Proline-Containing Dipeptides: Improved Stereoinduction under Solvent-Free Conditions. *J. Org. Chem.* **2011**, *76* (5), 1464-1467.

(89) Kotani, S.; Hashimoto, S.; Nakajima, M. Chiral Phosphine Oxide BINAPO as a Lewis Base Catalyst for Asymmetric Allylation and Aldol Reaction of Trichlorosilyl Compounds. *Tetrahedron* **2007**, *63* (15), 3122-3132.

(90) Almaşi, D.; Alonso, D. A.; Balaguer, A. N.; Nájera, C. Water *versus* Solvent-Free Conditions for the Enantioselective Inter- and Intramolecular Aldol Reaction Employing L-Prolinamides and L-Prolinethioamides as Organocatalysts. *Adv. Synth. Catal.* **2009**, *351* (7-8), 1123-1131.

TOC and synopsis

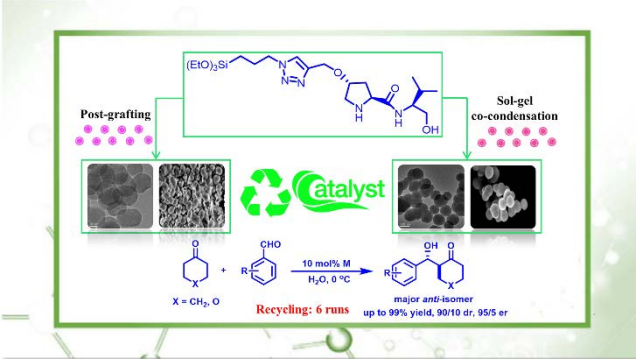

Mesoporous organosilica nanoparticles derived from proline-valinol amides as recyclable chiral organocatalysts for the direct asymmetric aldol reaction in water